

- T-lymphocyte proliferation. *Blood*. 2008;112(9):3788-3797.
43. Usui T, Yanagihara K, Tsukasaki K, et al. Characteristic expression of HTLV-1 basic zipper factor (HBZ) transcripts in HTLV-1 provirus-positive cells. *Retrovirology*. 2008;5:34.
44. Saito M, Matsuzaki T, Satou Y, et al. In vivo expression of the HBZ gene of HTLV-1 correlates with proviral load, inflammatory markers and disease severity in HTLV-1 associated myelopathy/tropical spastic paraparesis (HAM/TSP). *Retrovirology*. 2009;6:19.
45. Afonso PV, Mekaouche M, Mortreux F, et al. Highly active antiretroviral treatment against HTLV-1 infection combining reverse transcriptase and HDAC inhibitors. *Blood*. 2010;116(19):3802-3808.
46. Macnamara A, Rowan A, Hilburn S, et al. HLA class I binding of HBZ determines outcome in HTLV-1 infection. *PLoS Pathog*. 2010;6(9):e1001117.
47. Lagneaux L, Gillet N, Stamatopoulos B, et al. Valproic acid induces apoptosis in chronic lymphocytic leukemia cells through activation of the death receptor pathway and potentiates TRAIL response. *Exp Hematol*. 2007;35(10):1527-1537.
48. Kuendgen A, Gattermann N. Valproic acid for the treatment of myeloid malignancies. *Cancer*. 2007;110(5):943-954.
49. Mori N, Matsuda T, Tadano M, et al. Apoptosis induced by the histone deacetylase inhibitor FR901228 in human T-cell leukemia virus type 1-infected T-cell lines and primary adult T-cell leukemia cells. *J Virol*. 2004;78(9):4582-4590.
50. Chen J, Zhang M, Ju W, Waldmann TA. Effective treatment of a murine model of adult T-cell leukemia using depsipeptide and its combination with unmodified daclizumab directed toward CD25. *Blood*. 2009;113(6):1287-1293.
51. Nishioka C, Ikezoe T, Yang J, et al. Histone deacetylase inhibitors induce growth arrest and apoptosis of HTLV-1-infected T-cells via blockade of signaling by nuclear factor kappaB. *Leuk Res*. 2008;32(2):287-296.

Reduced Tim-3 Expression on Human T-lymphotropic Virus Type I (HTLV-I) Tax-specific Cytotoxic T Lymphocytes in HTLV-I Infection

Nashwa H. Abdelbary,¹ Hazem M. Abdullah,¹ Toshio Matsuzaki,² Daisuke Hayashi,² Yuetsu Tanaka,³ Hiroshi Takashima,² Shuji Izumo,¹ and Ryuji Kubota¹

¹Division of Molecular Pathology, Center for Chronic Viral Diseases and ²Department of Neurology and Geriatrics, Graduate School of Medical and Dental Sciences, Kagoshima University, 8-35-1 Sakuragaoka, Kagoshima, Japan; and ³Department of Immunology, Graduate School and Faculty of Medicine, University of the Ryukyus, Uehara 207, Nishihara-cho, Okinawa, Japan

T cell immunoglobulin and mucin domain-containing molecule-3 (Tim-3) and programmed cell death-1 (PD-1) are T cell exhaustion molecules. We investigated the expression of Tim-3 and PD-1 in human T-lymphotropic virus type I (HTLV-I) infection. Tim-3 expression, but not PD-1 expression, was reduced on CD4⁺ and CD8⁺ T cells of HTLV-I-associated myelopathy/tropical spastic paraparesis (HAM/TSP) patients and HTLV-I carriers as compared with healthy controls. Tim-3 expression was also reduced in HTLV-I Tax-specific cytotoxic T lymphocytes (CTLs) as compared with cytomegalovirus-specific CTLs. Tim-3⁺, but not PD-1⁺, Tax-specific CTLs produced less interferon- γ and exhibited low cytolytic activity. However, we observed no difference in the expression of Tim-3 or cytolytic activity between Tax-specific CTLs of HAM/TSP patients or carriers. Moreover, HTLV-I-infected CD4⁺ T cells showed decreased Tim-3 expression. These data suggest that Tim-3 expression is reduced in HTLV-I infection and that a high number of Tim-3⁺ HTLV-I-specific CTLs preserves their cytolytic activity, thereby controlling viral replication.

INTRODUCTION

Human T-lymphotropic virus type I (HTLV-I) is a retrovirus that preferentially infects CD4⁺ lymphocytes *in vivo* [1]. Although HTLV-I infection is lifelong, less than 1% of infected individuals develop HTLV-I-associated myelopathy/tropical spastic paraparesis (HAM/TSP), a neurologic disease, or adult T cell leukemia (ATL), a hematologic disease [2–4]. HAM/TSP is an inflammatory disease of the spinal cord characterized by infiltration of inflammatory cells into

the perivascular area [5]. Patients with HAM/TSP show spastic paraparesis and sphincter dysfunction with mild sensory disturbance [6]. HTLV-I proviral load and frequency of HTLV-I-specific CD8⁺ cytotoxic T lymphocytes (CTLs) are higher in the peripheral blood of patients with HAM/TSP as compared with asymptomatic carriers [7–9]. Although increasing evidence supports the hypothesis that such a strong CTL response could certainly contribute to the control of viral replication and disease development, the exact pathogenic role of the CTL responses remains unclear [10].

The T-cell receptor costimulatory pathways assist in regulating T cell activation or tolerance [11, 12]. Recently, programmed cell death-1 (PD-1) signaling was shown to play an important role in T cell exhaustion during chronic viral infections [13–16]. T cell immunoglobulin and mucin domain-containing molecule-3 (Tim-3) has been similarly associated with T cell exhaustion [17]. Interaction of Tim-3 with its ligand galectin-9 regulates Th1 cell responses by promoting the

Received 13 July 2010; accepted 15 November 2010.

Potential conflicts of interest: none reported.

Reprints or correspondence: Ryuji Kubota, MD, Division of Molecular Pathology, Center for Chronic Viral Diseases, Graduate School of Medical and Dental Sciences, Kagoshima University, 8-35-1 Sakuragaoka, Kagoshima 890-8544, Japan (E-mail: kubotar@m2.kufm.kagoshima-u.ac.jp).

The Journal of Infectious Diseases 2011;203:948–59

© The Author 2011. Published by Oxford University Press on behalf of the Infectious Diseases Society of America. All rights reserved. For Permissions, please e-mail: journals.permissions@oup.com
1537-6613/2011/2037-0001\$15.00
DOI: 10.1093/infdis/jiq153

death of interferon- γ (IFN- γ)-producing Th1 cells [18]. A recent study of human immunodeficiency virus (HIV) and hepatitis C virus (HCV) infections demonstrated that Tim-3 is upregulated in CD4⁺ and CD8⁺ T cells of patients with chronic viral infection. Tim-3-expressing T cells secrete less IFN- γ than do Tim-3-negative cells [19, 20]. In addition, a reduction of Tim-3 expression in T cells by using small interfering RNA or blocking antibodies increases the secretion of the antiviral cytokine IFN- γ [20, 21]. However, it is unclear whether T cells are exhausted or Tim-3 expression is upregulated in HTLV-I infection.

It remains unknown why only a small number of HTLV-I-infected individuals develop HAM/TSP, while the majority of the infected persons remain disease-free. It has been clearly demonstrated that elevated HTLV-I proviral loads increase the risk of HAM/TSP development [7, 22]. In addition, HAM/TSP patients have more HTLV-I-specific CTLs than do asymptomatic carriers [8, 23]. Recently, it has been postulated that CTLs in HAM/TSP patients have impaired function in association with degranulation of cytolytic molecules as compared with CTLs in asymptomatic carriers, which may result in an insufficient control of the virus [24]. However, it remains unclear whether CTL function is impaired in HAM/TSP patients.

In this study, we investigated Tim-3 and PD-1 expression in HTLV-I infection. In particular, we studied HTLV-I-specific CTLs and their degranulation activity in HAM/TSP patients and asymptomatic carriers as well as the role of Tim-3 and PD-1 in regulating their function.

MATERIALS AND METHODS

Patients

The study subjects consisted of 32 HAM/TSP patients, 31 asymptomatic carriers, and 11 uninfected healthy controls (Table 1). All subjects were residents of Kagoshima Prefecture, Japan. HTLV-I infection was determined using a HTLV-I antibody serological test, and HAM/TSP was diagnosed according to World Health Organization guidelines. All patients gave their written informed consent to participate in this study. Peripheral blood mononuclear cells (PBMCs) were separated from heparinized blood by Ficoll gradient centrifugation and stored in liquid nitrogen until use. To investigate HTLV-I-specific CTLs,

we selected HLA-A*0201-positive or HLA-A*2402-positive cases because HTLV-I Tax11–19 and Tax301–309 are well characterized and strong immunodominant epitopes are restricted to these HLAs [25–27]. This study was reviewed and approved by the Kagoshima University Ethical Committee.

Cell Surface Staining

After thawing, 1×10^6 PBMCs were stained with a rat IgG2a anti-Tim-3 antibody (R&D Systems). The cells were washed with a staining buffer (PBS containing 5% normal goat serum and 0.1% NaN₃) and further stained with a goat anti-rat IgG–Alexa Fluor 488 secondary antibody (Invitrogen). Alternatively, the cells were stained with an anti-PD-1–fluorescein isothiocyanate (FITC) (eBioscience), anti-CD3–energy-coupled dye (ECD), anti-CD4–phycoerythrin (PE)–Cy5 (PC5), or anti-CD8–PC5 antibody (Beckman Coulter), and a PE-labeled tetramer. The HLA/antigen tetramers used were as follows: HLA-A*0201/HTLV-I Tax11–19 (LLFGYPVYV), HLA-A*0201/CMV pp65 (NLVPMVATV), HLA-A*0201/HIV Gag (SLYNTVATL), HLA-A*2402/HTLV-I Tax301–309 (SFHSLHLLF), HLA-A*2402/CMV pp65 (QYDP-VAALF), and HLA-A*2402/HIV Gag (RYLKDQQLL) (Medical & Biological Laboratories). Alternatively, the cells were stained with anti-PD-L1–PE (eBioscience), anti-CD3–ECD, CD4–PC5 and CD8–FITC antibody (Beckman Coulter). Appropriate isotype antibodies were used as controls. Fluorescent signal was detected by an Epics XL flow cytometer, and Expo32 software was used for data acquisition and analysis (Beckman Coulter).

Intracellular IFN- γ Detection

PBMCs were cultured in complete medium (RPMI 1640 medium supplemented with 100 U/mL penicillin, 0.1 mg/mL streptomycin, and 10% heat-inactivated fetal cow serum) in the absence or presence of phorbol 12-myristate 13-acetate (PMA [5 ng/mL]) and ionomycin (0.5 μ g/mL) with 5 μ g/mL of the secretion inhibitor brefeldin A (Sigma) for 6 hours. After harvesting, the cells were stained with a rat anti-Tim-3 antibody, followed by staining with a goat anti-rat IgG–PC5 secondary antibody (Santa Cruz Biotechnology), or with an anti-PD-1–FITC antibody. The cells were then stained with an anti-CD8–ECD antibody (Beckman Coulter) and Tax tetramer–PE. The cells were fixed with 1% paraformaldehyde, resuspended in 50 μ L permeabilization buffer (0.1% saponin in staining buffer),

Table 1. Clinical Characteristics of the Study Groups

Subject	Number	Age (mean [SD])	Sex (M/F) ^a	HTLV-I proviral load ^b mean (SD)
HAM/TSP ^c	32	34–73 (57.8 [10.8])	11/21	2091.6 (3606.9)
Asymptomatic carrier	31	22–78 (55.3 [11.6])	10/21	608.9 (1159.9)
Healthy control	11	36–66 (49.4 [9.7])	1/10	N/A ^d

NOTE. ^a M/F: male/female.

^b copies/10⁴ cells.

^c HAM/TSP: HTLV-I-associated myelopathy/tropical spastic paraparesis.

^d N/A: not applicable.

and stained with an anti-IFN- γ -FITC antibody (Immunotech). For PD-1 detection, the cells were stained with anti-IFN- γ -biotin (eBioscience) followed by staining with a streptavidin-PC5 secondary antibody (Becton Dickinson). At least 3×10^5 CD8⁺ cells were examined by flow cytometry.

CD107a Degranulation Assay

Cytolytic activity was assessed by flow cytometric quantification of the surface mobilization of CD107a (cluster of differentiation 107a, an integral membrane protein in cytolytic granules) [28]. PBMCs (1×10^6) from patients with HLA-A*02 were pulsed with 1 μ M HTLV-I Tax11–19 or with the control influenza virus M1 peptide (GILGFVFTL) for 30 minutes; PBMCs from HLA-A*24 patients were pulsed with 1 μ M HTLV-I Tax301–309 or with HIV Gag (RYLKDQQL) peptide. Excess peptides were washed out and the cells were incubated with an anti-CD107a-PC5 antibody (Becton Dickinson [4 μ L/mL]) in the presence of brefeldin A (5 μ g/mL) for 4 hours. After harvesting, the cells were stained with a rat anti-Tim-3 antibody followed by an anti-rat IgG–Alexa Fluor 488 secondary antibody, or with an anti-PD-1–FITC antibody followed by staining with Tax tetramer–PE and an anti-CD8–ECD antibody. At least 1×10^5 CD8⁺ T cells were examined by flow cytometry.

Quantitative Polymerase Chain Reaction of the HTLV-I Proviral Load

Genomic DNA was extracted from PBMCs by using the Qiagen DNA extraction kit (Qiagen). The measurements were performed as described elsewhere [7].

Intracellular HTLV-I Tax Staining

PBMCs (5×10^5) were cultured for 12 hours in complete medium in the presence of brefeldin A. After harvesting, the cells were stained with an anti-Tim-3 antibody followed by an Alexa Fluor 488-labeled secondary antibody, or with an anti-PD-1–FITC antibody and then stained with an anti-CD4–PC5 or anti-CD8–PC5 antibody. The cells were intracellularly stained with a mouse IgG3 anti-HTLV-I Tax antibody (clone Lt-4) [29] followed by a goat anti-mouse IgG3–PE antibody (Southern Biotech).

Statistical Analysis

Mann–Whitney *U* test, Wilcoxon signed-rank test, and Spearman's rank correlation test were performed using StatView software version 5.0 (SAS Institute). *P* values of less than .05 were considered significant.

RESULTS

Low Frequency of Tim-3⁺ Cells Within CD4⁺ and CD8⁺ T Cell Populations in HTLV-I Infection

Tim-3⁺ cells within the lymphocyte gate were greatly reduced in asymptomatic carriers and HAM/TSP patients as

compared with healthy controls (Figure 1A, upper row). We observed reduced frequencies of Tim-3-expressing CD3⁺CD4⁺ T cells in HTLV-I-infected individuals (mean [SD]: 2.59% [1.3%] for asymptomatic carriers and 2.62% [1.3%] for HAM/TSP patients) compared with those in healthy controls (3.72% [1.5%]) (*P* = .031 and *P* = .034, respectively [Figure 1B]). The same was observed on CD3⁺CD8⁺ T cells of infected individuals (7.19% [4.3%] for asymptomatic carriers and 7.54% [4.4%] for HAM/TSP patients) compared with those in healthy controls (10.6% [3.2%]) (*P* = .026 and *P* = .021, respectively [Figure 1B]). However, we observed increased mean fluorescent intensity (MFI) of Tim-3-expressing CD4⁺ and CD8⁺ T cells in asymptomatic carriers as compared with healthy controls (*P* = .0031 and *P* = .046, respectively [Figure 1C]). Conversely, we could not detect significant differences in Tim-3 expression (neither frequency nor MFI) on CD4⁺ or CD8⁺ T cells of HAM/TSP patients and asymptomatic carriers (Figures 1B and 1C). The frequency of Tim-3⁺ cells within CD4⁺ or CD8⁺ T cells did not correlate with HTLV-I proviral loads in HAM/TSP patients, asymptomatic carriers, or when both groups were combined (data not shown).

Low Expression of Tim-3 on HTLV-I Tax-specific CTLs as compared With That on Cytomegalovirus-specific CTLs in HTLV-I Infection

Tim-3 expression on antigen-specific CD8⁺ T cells was examined in 9 HLA-A*02 HAM/TSP patients using HLA/antigen tetramers, as shown in Figure 2A. We found significantly lower levels of Tim-3 on HTLV-I Tax-specific versus cytomegalovirus (CMV)-specific CTLs in HAM/TSP patients (*P* = .038 [Figure 2B]). The frequency of Tim-3-expressing Tax-specific CTLs was significantly lower than that in the total CD8⁺ T-cell population (*P* = .0077 [Figure 2B]). The frequencies of Tax-specific CTLs in HLA-A*02⁺ asymptomatic carriers were too low to reliably evaluate Tim-3 expression on these cells. Using PBMCs from 9 HAM/TSP patients and 10 asymptomatic carriers with HLA-A*24, we found that the frequency of Tim-3-expressing Tax-specific CTLs was also significantly lower than that in the total CD8⁺ T cell population (*P* = .0077 and *P* = .013, respectively [Figures 2C and 2D]). We attempted to assess Tim-3 expression on CMV tetramer⁺ cells in this HLA-A*24 group but the frequencies of CMV-specific CTLs were too small to reliably evaluate Tim-3 expression. As expected, the frequency of Tax-specific CTLs was higher in HAM/TSP patients than in asymptomatic carriers (Figure 2E). The frequency of Tim-3⁺ cells in Tax-specific CTLs was not different between the 2 groups (Figure 2F). However, the MFI of Tim-3 in Tax-specific CTLs was significantly higher in asymptomatic carriers than in HAM/TSP patients (*P* = .0084 [Figure 2G]). In addition, we detected no correlation between the frequency of Tim-3⁺ Tax-specific CTLs and HTLV-I proviral load, duration of illness, disease

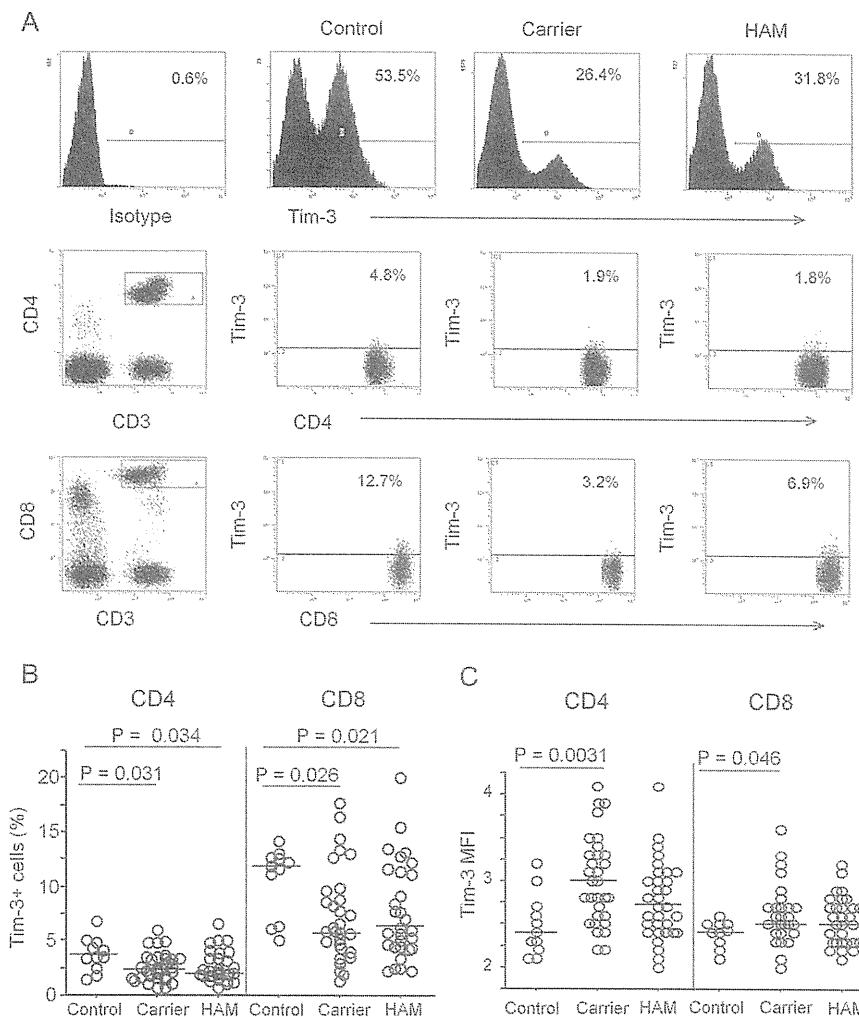


Figure 1. Low frequency of Tim-3⁺ cells within the CD4⁺ and CD8⁺ T cell populations in HTLV-I infection. PBMCs from 63 HTLV-I-infected (32 HAM/TSP patients and 31 carriers) and 11 uninfected subjects were stained with antibodies against CD3, CD4, or CD8 and Tim-3. The numbers indicate the percentage of Tim-3⁺ cells within each cell population. (A) Representative data from each group are shown in the last 3 columns. The upper row shows the expression levels of Tim-3 in total lymphocytes. The middle and lower rows show Tim-3 expression in CD3⁺CD4⁺ and CD3⁺CD8⁺ cells, respectively. (B) The combined data from all studied subjects reveal significantly lower percentages of Tim-3⁺ cells within CD4⁺ and CD8⁺ T cell populations of HAM/TSP patients and carriers than those of controls. Each symbol represents an individual subject, and the horizontal bars indicate the medians. Data were analyzed by Mann-Whitney *U* test. (C) The combined data from all studied subjects reveal significantly higher MFI of Tim-3⁺ cells in CD4⁺ and CD8⁺ T cell populations of carriers than those of controls. Data were analyzed by Mann-Whitney *U* test. Each symbol represents an individual subject, and the horizontal bars indicate the medians in each group.

NOTE: PBMCs: peripheral blood mononuclear cells; HAM/TSP: HTLV-I-associated myelopathy/tropical spastic paraparesis; Tim-3: T cell immunoglobulin and mucin domain-containing molecule-3; MFI: mean fluorescent intensity; HAM: HTLV-I-associated myelopathy/tropical spastic paraparesis.

activity, age of the patients, or serum HTLV-1 antibody titer (data not shown).

Increased PD-1 Expression on HTLV-I Tax-specific CTLs as Compared With That on CMV-specific CTLs

Since PD-1 has been also recognized as a marker for T cell exhaustion, we assessed PD-1 expression levels in 9 HAM/TSP patients, 8 asymptomatic carriers, and 10 healthy controls (Figure 3A). We could not detect a significant difference in PD-1 expression (neither frequency nor MFI) between HAM/TSP patients, asymptomatic carriers, and healthy controls in either

CD4⁺ or CD8⁺ T cells (Figure 3B). However, we observed a significantly higher frequency of PD-1-expressing Tax-specific CTLs in asymptomatic carriers as compared with that in HAM/TSP patients ($P = .043$ [Figure 3C]). We assessed PD-L1 expression levels in all three groups. Since expression levels were relatively small (0.07–0.76%) in either CD3⁺CD4⁺ or CD3⁺CD8⁺ cells, we did not consider these results. Next, we analyzed PD-1 expression on antigen-specific cells (Figure 3D) and found significantly higher PD-1 expression on Tax-specific CTLs as compared with CMV-specific CTLs ($P = .046$

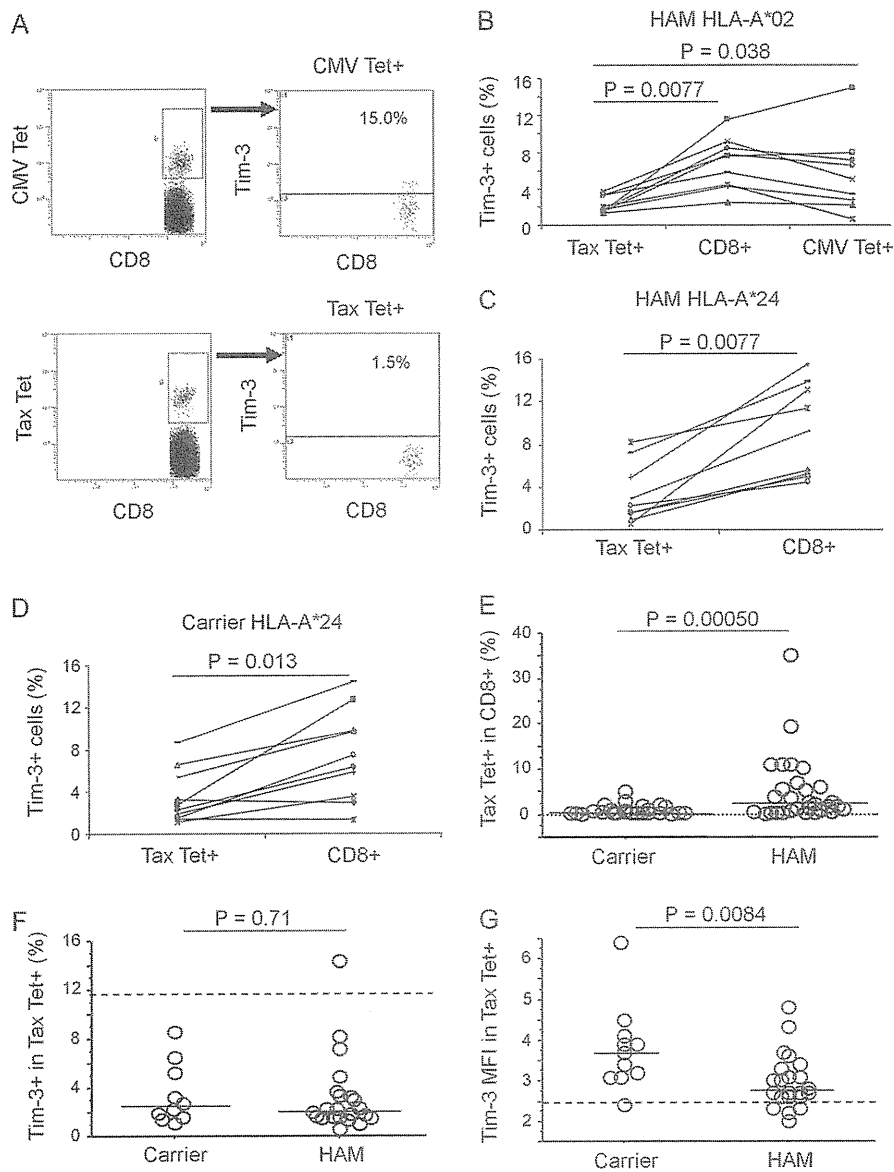


Figure 2. Low expression of Tim-3 on HTLV-I Tax-specific CTLs as compared with that on CMV-specific CTLs in HTLV-I infection. Tim-3 expression was determined in CD8⁺, CD8⁺Tax tetramer⁺, and CD8⁺CMV tetramer⁺ cells of HAM/TSP patients and carriers. (A) A representative flow cytometry analysis depicts Tim-3 expression on tetramer⁺ cells from a HAM/TSP patient. Gated CD8⁺tetramer⁺ cells were used for quantification of Tim-3⁺ cells. The upper and bottom rows show Tim-3 expression in CMV-specific and HTLV-I Tax-specific CTLs. The numbers indicate the percentage of Tim-3⁺ cells in each of the tetramer⁺ cell populations. (B) The combined data from 9 HLA-A*02⁺ HAM/TSP patients show significantly lower expression of Tim-3 in Tax-specific CTLs than in total CD8⁺ T cells or CMV-specific CTLs, by Wilcoxon signed-rank test. (C, D) The combined data from 9 HAM/TSP patients and 10 carriers, all HLA-A*24⁺, show significantly lower expression of Tim-3 in Tax-specific CTLs in comparison to total CD8⁺ T cells, by Wilcoxon signed-rank test. (E) The percentage of Tax tetramer⁺ cells within the CD8⁺ cell population in HAM/TSP patients and carriers is depicted. Patients have significantly higher number of Tax tetramer⁺ cells as compared with carriers, by Mann–Whitney *U* test. (F, G) Tim-3⁺ cells in CD8⁺Tax tetramer⁺ cells of HAM/TSP patients and carriers are shown. There is no significant difference in the frequency of Tim-3⁺ cells between the 2 groups. The carriers show significantly higher MFI of Tim-3 than do HAM/TSP patients. Data were analyzed by Mann–Whitney *U* test.

NOTE: In E–G, each symbol represents an individual subject and the horizontal bars indicate the medians in each group. In F and G, the dashed lines indicate the medians of Tim-3⁺ cells within the CD8⁺ cell population from healthy controls. Tim-3: T cell immunoglobulin and mucin domain-containing molecule-3; HAM/TSP: HTLV-I-associated myelopathy/tropical spastic paraparesis; CMV: cytomegalovirus; HTLV-I: human T-lymphotropic virus type I; CTLs: cytotoxic T lymphocytes; MFI: mean fluorescent intensity; HAM: HTLV-I-associated myelopathy/tropical spastic paraparesis; Tet: tetramer.

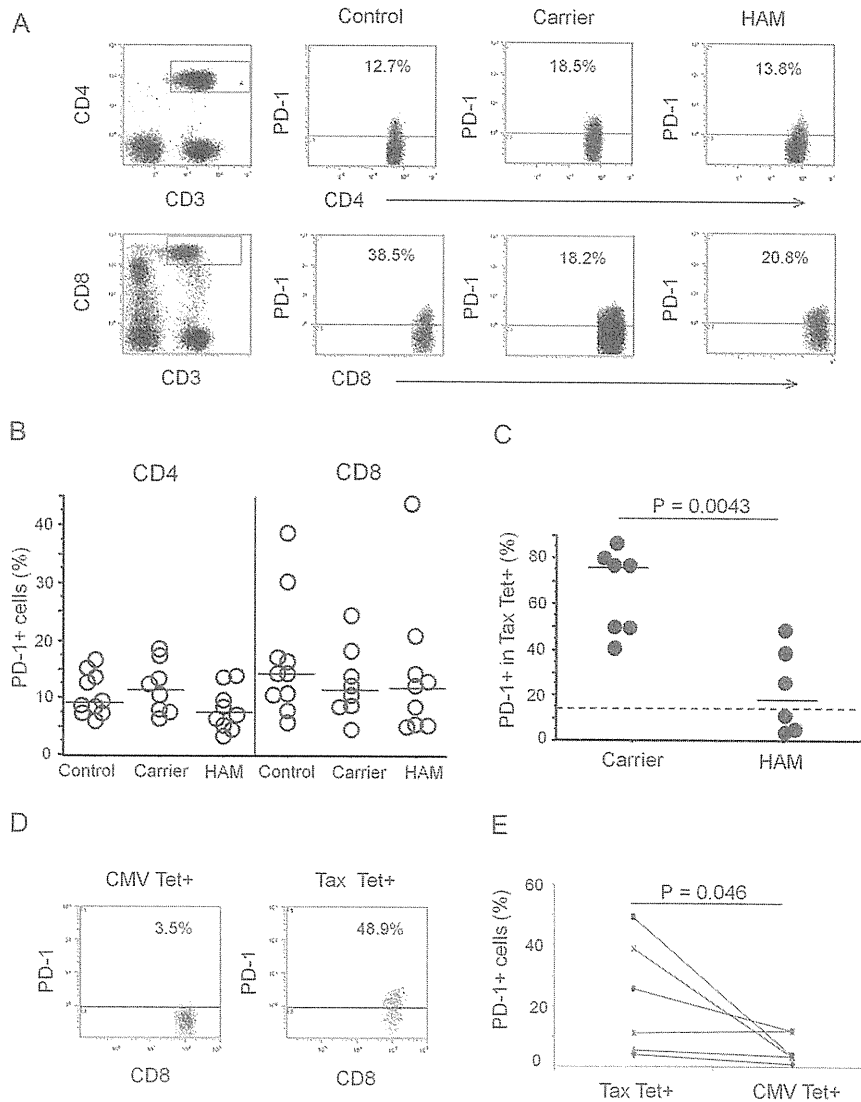


Figure 3. Increased PD-1 expression on HTLV-I Tax-specific CTLs as compared with that on CMV-specific CTLs. PD-1 expression was analyzed in PBMCs from 9 HAM/TSP patients, 8 carriers, and 10 controls after gating $CD3^+CD4^+$, $CD3^+CD8^+$, $CD8^+$ Tax tetramer $^+$, or $CD8^+$ CMV tetramer $^+$ cells. (A) The left column shows gated $CD3^+CD4^+$ and $CD3^+CD8^+$ cells. The last 3 columns show representative data of PD-1 expression in a control, a carrier, and a HAM/TSP patient after gating. (B) The combined data from all studied subjects show no significant difference in PD-1 expression between the 3 groups in $CD4^+$ or $CD8^+$ T cells, by Mann–Whitney *U* test. (C) The frequencies of PD-1 $^+$ cells within $CD8^+$ Tax tetramer $^+$ cells in HAM/TSP patients and carriers are shown. The carriers show significantly higher frequencies than HAM/TSP patients, by Mann–Whitney *U* test. The bars indicate the medians. The dashed line indicates the median value of PD-1 $^+$ cells within the $CD8^+$ cell population from healthy controls. (D) The plots depict representative PD-1 expression in either $CD8^+$ CMV tetramer $^+$ or $CD8^+$ Tax tetramer $^+$ cells. Tax tetramer $^+$ cells show higher PD-1 expression than CMV tetramer $^+$ cells. (E) The combined data from 6 HAM/TSP patients show significantly higher expression of PD-1 in Tax tetramer $^+$ cells than in CMV tetramer $^+$ cells, by Wilcoxon signed-rank test.

NOTE: PD-1: programmed cell death-1; PBMCs: peripheral blood mononuclear cells; HAM/TSP: HTLV-I-associated myelopathy/tropical spastic paraparesis; CMV: cytomegalovirus; HAM: HTLV-I-associated myelopathy/tropical spastic paraparesis; Tet: tetramer.

[Figure 3E]). We detected no correlation between the frequency of PD-1 $^+$ Tax-specific CTLs and HTLV-I proviral load, duration of illness, disease activity, age of the patients, or serum HTLV-I antibody titer (data not shown). For technical reasons, we could not establish a double staining protocol for Tim-3 and PD-1.

Reduced IFN- γ Production by Tim-3 $^+$ HTLV-I Tax-specific CTLs

We compared IFN- γ production after PMA/ionomycin stimulation between Tim-3 $^+$ and Tim-3 $^-$ cells, or PD-1 $^+$ and PD-1 $^-$

cells, within $CD8^+$ or Tax-specific CTL populations. As shown in Figures 4A and 4D, we determined the percentage of IFN- γ^+ cells after gating on either $CD8^+$ or $CD8^+$ Tax tetramer $^+$ cells from HAM/TSP patients with a high percentage of tetramer $^+$ cells. IFN- γ was predominately produced by Tim-3 $^-$ cells, and less by Tim-3 $^+$ cells in both groups (Figures 4B and 4C). Statistical analysis showed a significant difference in IFN- γ production (frequency and MFI) within $CD8^+$ cells ($P = .043$ and $.043$,

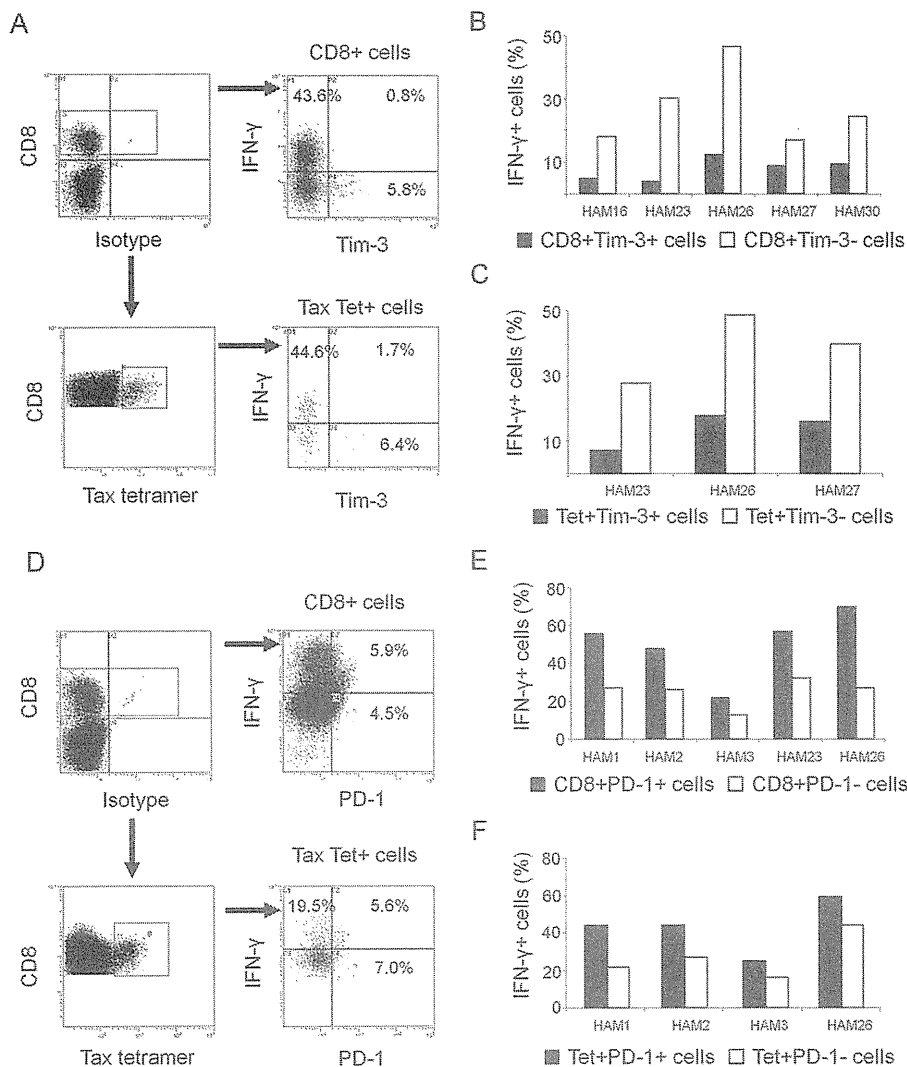


Figure 4. Reduced IFN- γ production by Tim-3⁺ HTLV-I Tax-specific CTLs. PBMCs from 5 HAM/TSP patients were stimulated with PMA and ionomycin, and cultured for 6 hours in the presence of brefeldin A. IFN- γ production was determined by flow cytometry in CD8⁺ and CD8⁺Tax tetramer⁺ cells with or without Tim-3 or PD-1 expression. (A, D) Representative data from a HAM/TSP patient are shown. The upper and lower rows show the percentage of IFN- γ ⁺ cells in gated CD8⁺ and CD8⁺Tax tetramer⁺ cell populations, respectively. In A, Tim-3⁺ cells within CD8⁺ and Tax tetramer⁺ cell populations have a lower percentage of IFN- γ ⁺ cells than do Tim-3⁻ cells. In D, PD-1⁺ cells within CD8⁺ and Tax tetramer⁺ cell populations have a higher percentage of IFN- γ ⁺ cells than do PD-1⁻ cells. (B) Summary data from 5 HAM/TSP patients show a significantly lower percentage of IFN- γ ⁺ cells within the CD8⁺Tim-3⁺ cell population than within the CD8⁺Tim-3⁻ one, after background subtraction ($P = .043$ by Wilcoxon signed-rank test). (C) Summary data from 3 HAM/TSP patients with high percentage of CTLs show a lower percentage of IFN- γ ⁺ cells within the Tax tetramer⁺Tim-3⁺ cell population than within the Tax tetramer⁺Tim-3⁻ one, after background subtraction. (E) Summary data from 5 HAM/TSP patients show a significantly higher percentage of IFN- γ ⁺ cells within the CD8⁺PD-1⁺ cell population than within the CD8⁺PD-1⁻ one ($P = .043$ by Wilcoxon signed-rank test). (F) Summary data from 4 HAM/TSP patients with high percentage of CTLs show a higher percentage of IFN- γ ⁺ cells within the Tax tetramer⁺PD-1⁺ cell population than within the Tax tetramer⁺PD-1⁻ one.

NOTE: PBMCs: peripheral blood mononuclear cells; HAM/TSP: HTLV-I-associated myelopathy/tropical spastic paraparesis; PMA: phorbol 12-myristate 13-acetate; IFN- γ : interferon- γ ; Tim-3: T cell immunoglobulin and mucin domain-containing molecule-3; PD-1: programmed cell death-1; CTLs: cytotoxic T lymphocytes; Tet: tetramer.

respectively). Conversely, IFN- γ was predominately produced by PD-1⁺ cells and less by PD-1⁻ cells in both groups (Figures 4E and 4F). Statistical analysis showed a significant difference in IFN- γ production within CD8⁺ cells, as measured by frequency ($P = .043$). However, no difference was observed in the MFI.

Reduced CD107a Expression on Tim-3⁺ HTLV-I Tax-specific CTLs

To assess the cytolytic activity of HTLV-I Tax-specific CTLs with or without Tim-3 or PD-1 expression, we measured CD107a expression after specific peptide stimulation of Tax-specific

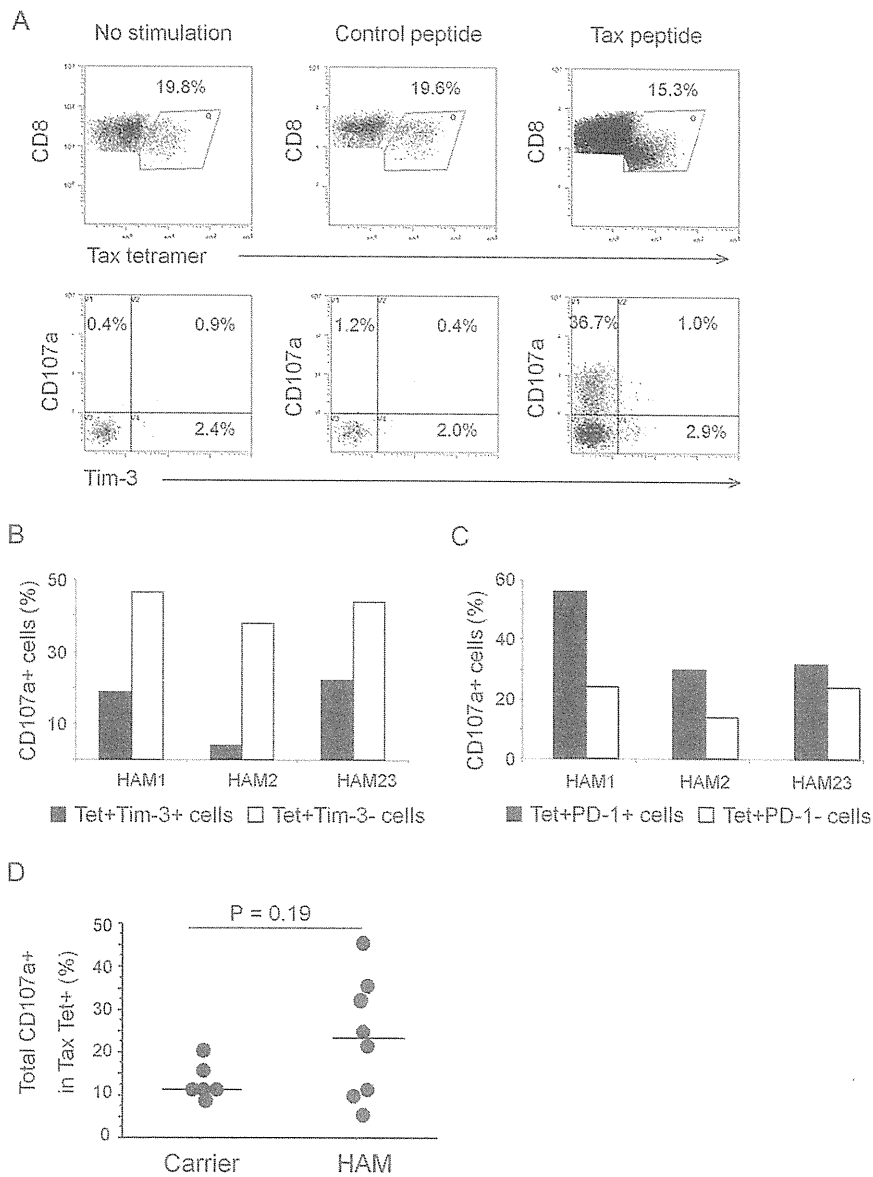


Figure 5. Reduced CD107a expression on Tim-3⁺ HTLV-I Tax-specific CTLs. PBMCs from 8 HAM/TSP patients and 6 carriers were stimulated with HTLV-I Tax peptide or a control peptide, and cultured in the presence of an anti-CD107a antibody and brefeldin A for 4 hours. The expression of CD107a on CD8⁺Tax tetramer⁺ cells was analyzed. (A) Representative data from a HAM/TSP patient are shown. In the upper row, Tax peptide-stimulated Tax tetramer⁺ cells show a parallel decrease in fluorescence intensity for CD8 and Tax tetramer. The same was not observed with the control peptide. The percentage of tetramer⁺ cells is reduced after Tax peptide stimulation. In the lower row, the frequency of CD107a-expressing cells is analyzed in tetramer⁺Tim-3⁺ and tetramer⁺Tim-3⁻ cells. Tetramer⁺Tim-3⁺ cells show a lower percentage of CD107a⁺ cells than tetramer⁺Tim-3⁻ cells. (B, C) Three HAM/TSP patients from whom more than 10⁴ Tax-tetramer⁺ cells could be collected were chosen for a precise evaluation. (B) The summary data show low CD107a expression in tetramer⁺Tim-3⁺ cells in comparison with tetramer⁺Tim-3⁻ cells, after background subtraction. (C) The summary data show high CD107a expression in tetramer⁺PD-1⁺ cells in comparison to tetramer⁺PD-1⁻ cells. (D) The percentage of CD107a⁺ cells within Tax tetramer⁺ cells from 8 HAM/TSP patients and 6 carriers is shown. No significant difference was observed in the percentage of CD107a⁺ cells between the 2 groups ($P = .19$ by Mann-Whitney U test). The bars indicate the medians.

NOTE: PBMCs: peripheral blood mononuclear cells; HAM/TSP: HTLV-I-associated myelopathy/tropical spastic paraparesis; HTLV-I: human T-lymphotropic virus type I; CD107a: cluster of differentiation 107a; HAM: HTLV-I-associated myelopathy/tropical spastic paraparesis; Tet: tetramer.

CTLs from 8 HAM/TSP patients and 6 asymptomatic carriers. Representative data from a HAM/TSP patient are shown in Figure 5A. Specific antigen-induced CD107a expression was higher in tetramer⁺Tim-3⁻ cells than in tetramer⁺Tim-3⁺

cells. At the same time, CD107a expression was higher in tetramer⁺PD-1⁺ cells than in tetramer⁺PD-1⁻ cells from 3 HAM/TSP patients from whom we could collect more than 10⁴ tetramer⁺ cells for a more precise evaluation (Figures 5B and 5C).

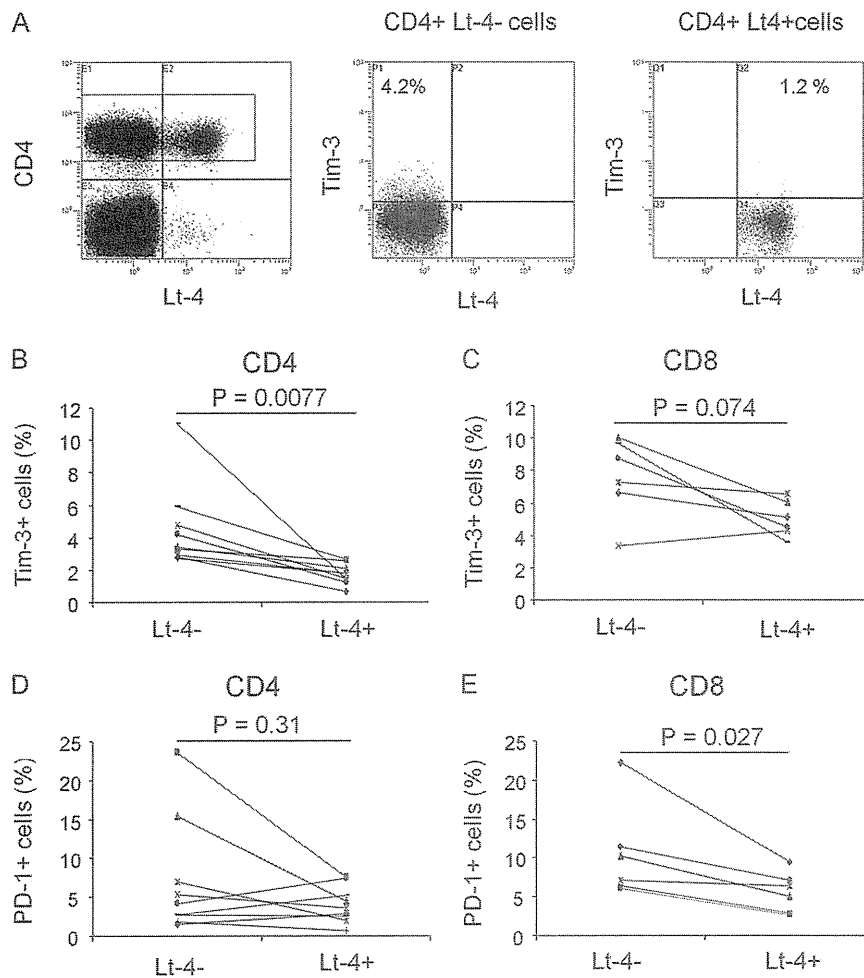


Figure 6. Low expression of Tim-3 on HTLV-I-infected cells. PBMCs from 9 HAM/TSP patients were cultured for 12 hours. Cells were double stained for the intracellular HTLV-I Tax protein, using the Lt-4 antibody, and the cell surface Tim-3 or PD-1. (A) After gating on CD4⁺ cells, expression of Tim-3 was analyzed in either CD4⁺Lt-4⁺ or CD4⁺Lt-4⁻ cells. Representative data from a HAM/TSP patient show low percentage of Tim-3⁺ cells in CD4⁺Lt-4⁺ cells in comparison to CD4⁺Lt-4⁻ cells. (B, D) Combined data from 9 HAM/TSP patients show significantly lower Tim-3 expression in CD4⁺Lt-4⁺ cells than in CD4⁺Lt-4⁻ cells. No significant difference in PD-1 expression between both groups was found by Wilcoxon signed-rank test. (C, E) Combined data from 6 HAM/TSP patients show that Tim-3 expression tended to be lower in CD8⁺Lt-4⁺ cells than in CD8⁺Lt-4⁻ cells and that PD-1 expression was significantly lower in CD8⁺Lt-4⁺ cells than in CD8⁺Lt-4⁻ cells, by Wilcoxon signed-rank test.

NOTE: PBMCs: peripheral blood mononuclear cells; HAM/TSP: HTLV-I-associated myelopathy/tropical spastic paraparesis; HTLV-I: human T-lymphotropic virus type I; Tim-3: T cell immunoglobulin and mucin domain-containing molecule-3; PD-1: programmed cell death-1.

Furthermore, when we reanalyzed the frequency or MFI of CD107a⁺ cells within the Tax tetramer⁺ cell population, we could not detect a significant difference between HAM/TSP patients and asymptomatic carriers (Figure 5D). Also, we could not detect a significant correlation between the frequency of CD107a⁺ cells and HTLV-I proviral load (data not shown).

Low Expression of Tim-3 on CD4⁺ HTLV-I-infected Cells

To assess Tim-3 expression on HTLV-I-infected cells, we cultured PBMCs from 9 HAM/TSP patients for 12 hours in order to induce the expression of the HTLV-I Tax protein [30]. After harvesting, Tax protein was simultaneously detected with Tim-3 or PD-1 (Figure 6A). We observed that

Tim-3 expression was significantly lower in Tax⁺ CD4⁺ cells (Lt-4⁺ cells) than in Tax⁻CD4⁺ cells ($P = .0077$ [Figure 6B]). On the contrary, we observed no significant differences in PD-1 expression between Tax⁺CD4⁺ and Tax⁻CD4⁺ cells ($P = .31$ [Figure 6D]). In addition, we assessed the expression of Tim-3 or PD-1 in infected CD8⁺ cells from 6 cases that showed a reasonable percentage of infected CD8⁺ cells. We found that Tim-3 expression tended to be lower in Tax⁺CD8⁺ cells than in Tax⁻CD8⁺ cells ($P = .074$ [Figure 6C]), whereas PD-1 expression was significantly lower in Tax⁺CD8⁺ cells than in Tax⁻CD8⁺ cells ($P = .027$ [Figure 6E]). No significant correlations were observed between the MFI of Lt-4-positive cells and the frequency or

MFI of Tim-3 or PD-1 within CD4⁺ or CD8⁺ cells (data not shown). The percentage of infected CD4⁺ and CD8⁺ cells in asymptomatic carriers or tetramer⁺CD8⁺ cells in HAM/TSP patients was too small to assess Tim-3 or PD-1 expression.

CONCLUSIONS

We found that the proportion of Tim-3⁺ cells within CD4⁺ and CD8⁺ T cell populations of HTLV-I-infected individuals (both HAM/TSP patients and asymptomatic carriers) is significantly lower than in healthy controls (Figure 1). This reduction was much clearer in Tax-specific CTLs because the frequency of Tim-3-expressing cells in CTLs was lower than in the total CD8⁺ population of infected individuals (Figures 2B–D). In addition, Tim-3⁺ cell frequency in HTLV-I Tax-specific CTLs was significantly lower than in CMV-specific CTLs from HAM/TSP patients (Figure 2B). Interaction of Tim-3 with its ligand, galectin-9, regulates Th1 cell responses by promoting the death of IFN- γ -producing Th1 cells, suggesting that Tim-3 may play a role in suppressing Th1-mediated immune responses [18]. Our results showing that the frequency of Tim-3⁺ cells is reduced within CD4⁺ and CD8⁺ T cells in HTLV-I infection strongly suggest that the Th1/Tc1 immune response is not negatively regulated by Tim-3 in HTLV-I infection. Rather, immune cells such as HTLV-I-specific CTLs may be resistant to cell death through the Tim-3/galectin-9 pathway [18]. In this sense, the increased number of Tim-3⁺ HTLV-I Tax-specific CTLs may contribute to the control of viral replication. In the present study, we found that IFN- γ production was decreased in CD8⁺ cells and HTLV-I Tax-specific CTLs that expressed Tim-3 as compared with their Tim-3⁻ counterparts in HAM/TSP patients (Figure 4). In addition, CD107a expression was lower in Tim-3⁺ HTLV-I Tax-specific CTLs from HAM/TSP patients (Figure 5). These results indicate that Tim-3 identifies a subset of CTLs with impaired production of cytokines and cytolytic activity. The decreased expression of Tim-3 in HTLV-I infection is in marked contrast to other chronic viral infections such as HIV and HCV infections, where Tim-3 expression is increased in T cells, including the virus-specific CTLs [19, 20]. It would be of interest to determine whether Tim-3 expression is also reduced in other chronic viral infections and to clarify the mechanisms underlying Tim-3 down-regulation in HTLV-I infection.

Interestingly, our data demonstrated that Tim-3 and CD107a expression in HTLV-I Tax-specific CTLs was not significantly different between HAM/TSP patients and asymptomatic carriers (Figures 2F and 5D); however, Tim-3 MFI was higher in asymptomatic carriers than in HAM/TSP patients. Our data suggest that the killing activity of the CTLs is not different between the 2 groups. Controversially, others have reported that CD107a expression is lower in HTLV-I Tax-specific CTLs from HAM/TSP patients than from asymptomatic carriers, and that CTL function is impaired in HAM/TSP patients as compared with

asymptomatic carriers [24]. This controversy may result from differences in sample type and procedures, including the gating for tetramer⁺ cells after antigen stimulation. To address this issue, more detailed analyses of HTLV-I-specific CTL function in HAM/TSP patients and asymptomatic carriers would be necessary to ascertain whether differences could define the clinical condition.

In this study, we found that PD-1 expression levels on T cells of HAM/TSP patients and asymptomatic carriers were not different from those of healthy controls. However, we observed that PD-1 expression was significantly higher in HTLV-I Tax-specific CTLs than in CMV-specific CTLs (Figure 3E) and significantly higher in HTLV-I Tax-specific CTLs from asymptomatic carriers than from HAM/TSP patients. This result is in partial agreement with a previous study on HTLV-I infection, in which a marked increase of PD-1 expression was found in HTLV-I Tax-specific CTLs from both asymptomatic carriers and ATL patients as compared with CMV- and EBV-specific CTLs [31]. We found that IFN- γ production was higher in CD8⁺ cells and HTLV-I Tax-specific CTLs that expressed PD-1 as compared with their PD-1⁻ counterparts in HAM/TSP patients (Figures 4E and 4F). In addition, CD107a expression was higher in PD-1⁺ HTLV-I Tax-specific CTLs of HAM/TSP patients (Figure 5C). These results indicate that PD-1⁺ HTLV-I Tax-specific CTLs are capable of producing proinflammatory cytokines and have high cytolytic activity during HTLV-I infection. An increase in IFN- γ production by PD-1⁺ T cells has been recently shown in simian immunodeficiency virus (SIV) infection and in an animal model of autoimmune nephritis [32, 33]. Interestingly, PD-1⁺ cells were predominantly detected within CD107a⁺ antigen-specific T cells in SIV infection [34]. In this context, it is proposed that the primary mechanism by which PD-1 affects CD8⁺ T cell function involves regulation of cell proliferation and survival [32, 35]. Our results suggest that HTLV-I Tax-specific CTLs exhibit an increased expression of PD-1, albeit a reduced expression of Tim-3. This is in marked contrast to other chronic viral infections such as HIV and HCV infections, in which both PD-1 and Tim-3 are expressed at high levels in the virus-specific CTLs [19, 20]. Double staining for Tim-3 and PD-1 revealed that these are expressed by distinct populations of CD8⁺ T cells in HIV infection and that the predominance of either Tim-3⁺PD-1⁻ or Tim-3⁻PD-1⁺ cells in HIV-specific CTLs differs among individuals [19]. At the same time, CMV- and HCV-specific CTLs are predominantly Tim-3⁻PD-1⁺ and Tim-3⁺PD-1⁺, respectively [20]. In our study, the average percentage of PD-1⁺ cells in HTLV-I Tax-specific CTLs was 65.9% and 22.3% in carriers and HAM/TSP patients, respectively (Figure 3C); the average percentage of Tim-3⁺ cells was 3.5% and 3.2%, respectively (Figure 2F), suggesting that the majority of the CTLs expressing T cell exhaustion molecules has a Tim-3⁻PD-1⁺ phenotype. Taken together, these results suggest that PD-1 and Tim-3 may have a distinct function in regulating immune responses in HTLV-I infection.

We observed that HTLV-I Tax-expressing cells show a significant reduction in Tim-3 expression as compared with Tax⁻CD4⁺ cells and that Tim-3 expression in Tax⁺CD8⁺ cells tends to be lower than in Tax⁻CD8⁺ cells. Tax⁺CD8⁺ cells also showed significantly lower PD-1 expression (Figure 6). This suggests that HTLV-I-infected cells may be resistant to cell death through the Tim-3/galectin-9 pathway. HTLV-I Tax combines a positive effect on cell cycle with a negative effect on apoptosis through transactivation of several host genes [36]. It would be of interest to further investigate whether Tax might regulate Tim-3 expression.

In summary, we demonstrated that the expression of the negative immune regulator Tim-3, but not of PD-1, is reduced on HTLV-I Tax-specific CTLs, CD4⁺, and CD8⁺ T cells in both HAM/TSP patients and asymptomatic carriers. Moreover, we showed that Tim-3⁺, but not PD-1⁺, cells produce less IFN- γ and exhibit low cytolytic activity within the CTL population. Tim-3 expression and CTL cytolytic activity were not different between HAM/TSP patients and asymptomatic carriers. In addition, CD4⁺ HTLV-I Tax-expressing cells showed a significant reduction in Tim-3 expression as compared with Tax⁻CD4⁺ cells. These results suggest that HTLV-I Tax-specific CTLs preserve their cytolytic activity, thereby controlling viral replication.

Funding

Grant-in-Aid for Research on Brain Science from the Ministry of Health, Labor and Welfare, Japan, and Grant-in-Aid for Scientific Research from the Ministry of Education, Culture, Sports, Science and Technology, Japan.

Acknowledgments

We thank Ms. Takako Inoue for the excellent technical assistance.

References

- Richardson JH, Edwards AJ, Cruickshank JK, Rudge P, Dalgleish AG. In vivo cellular tropism of human T-cell leukemia virus type 1. *J Virol* 1990; 64:5682–7.
- Uchiyama T, Yodoi J, Sagawa K, Takatsuki K, Uchino H. Adult T-cell leukemia: clinical and hematologic features of 16 cases. *Blood* 1977; 50:481–92.
- Gessain A, Barin F, Vernant JC, et al. Antibodies to human T-lymphotropic virus type-I in patients with tropical spastic paraparesis. *Lancet* 1985; 2:407–10.
- Osame M, Usuku K, Izumo S, et al. HTLV-I associated myelopathy, a new clinical entity. *Lancet* 1986; 1:1031–2.
- Umehara F, Izumo S, Nakagawa M, et al. Immunocytochemical analysis of the cellular infiltrate in the spinal cord lesions in HTLV-I-associated myelopathy. *J Neuropathol Exp Neurol* 1993; 52:424–30.
- Osame M, Matsumoto M, Usuku K, et al. Chronic progressive myelopathy associated with elevated antibodies to human T-lymphotropic virus type I and adult T-cell leukemia-like cells. *Ann Neurol* 1987; 21:117–22.
- Nagai M, Usuku K, Matsumoto W, et al. Analysis of HTLV-I proviral load in 202 HAM/TSP patients and 243 asymptomatic HTLV-I car-

- riers: high proviral load strongly predisposes to HAM/TSP. *J Neurovirol* 1998; 4:586–93.
- Jacobson S, Shida H, McFarlin DE, Fauci AS, Koenig S. Circulating CD8⁺ cytotoxic T lymphocytes specific for HTLV-I pX in patients with HTLV-I associated neurological disease. *Nature* 1990; 348:245–8.
- Greten TF, Slansky JE, Kubota R, et al. Direct visualization of antigen-specific T cells: HTLV-1 Tax11–19-specific CD8(+) T cells are activated in peripheral blood and accumulate in cerebrospinal fluid from HAM/TSP patients. *Proc Natl Acad Sci USA* 1998; 95:7568–73.
- Bangham CR, Osame M. Cellular immune response to HTLV-1. *Oncogene* 2005; 24:6035–46.
- Blank C, Mackensen A. Contribution of the PD-L1/PD-1 pathway to T-cell exhaustion: an update on implications for chronic infections and tumor evasion. *Cancer Immunol Immunother* 2007; 56:739–45.
- Sharpe AH, Wherry EJ, Ahmed R, Freeman GJ. The function of programmed cell death 1 and its ligands in regulating autoimmunity and infection. *Nat Immunol* 2007; 8:239–45.
- Okazaki T, Honjo T. Rejuvenating exhausted T cells during chronic viral infection. *Cell* 2006; 124:459–61.
- Barber DL, Wherry EJ, Masopust D, et al. Restoring function in exhausted CD8 T cells during chronic viral infection. *Nature* 2006; 439:682–7.
- Trautmann L, Janbazian L, Chomont N, et al. Upregulation of PD-1 expression on HIV-specific CD8⁺ T cells leads to reversible immune dysfunction. *Nat Med* 2006; 12:1198–202.
- D'Souza M, Fontenot AP, Mack DG, et al. Programmed death 1 expression on HIV-specific CD4⁺ T cells is driven by viral replication and associated with T cell dysfunction. *J Immunol* 2007; 179:1979–87.
- Hafler DA, Kuchroo V. TIMs: central regulators of immune responses. *J Exp Med* 2008; 205:2699–701.
- Zhu C, Anderson AC, Schubart A, et al. The Tim-3 ligand galectin-9 negatively regulates T helper type 1 immunity. *Nat Immunol* 2005; 6:1245–52.
- Jones RB, Ndhlovu LC, Barbour JD, et al. Tim-3 expression defines a novel population of dysfunctional T cells with highly elevated frequencies in progressive HIV-1 infection. *J Exp Med* 2008; 205:2763–79.
- Golden-Mason L, Palmer BE, Kassam N, et al. Negative immune regulator Tim-3 is overexpressed on T cells in hepatitis C virus infection and its blockade rescues dysfunctional CD4⁺ and CD8⁺ T cells. *J Virol* 2009; 83:9122–30.
- Koguchi K, Anderson DE, Yang L, O'Connor KC, Kuchroo VK, Hafler DA. Dysregulated T cell expression of TIM3 in multiple sclerosis. *J Exp Med* 2006; 203:1413–8.
- Vine AM, Witkover AD, Lloyd AL, et al. Polygenic control of human T lymphotropic virus type I (HTLV-I) provirus load and the risk of HTLV-I-associated myelopathy/tropical spastic paraparesis. *J Infect Dis* 2002; 186:932–9.
- Kubota R, Kawanishi T, Matsubara H, Manns A, Jacobson S. Demonstration of human T lymphotropic virus type I (HTLV-I) tax-specific CD8⁺ lymphocytes directly in peripheral blood of HTLV-I-associated myelopathy/tropical spastic paraparesis patients by intracellular cytokine detection. *J Immunol* 1998; 161:482–8.
- Sabouri AH, Usuku K, Hayashi D, et al. Impaired function of human T-lymphotropic virus type 1 (HTLV-1)-specific CD8⁺ T cells in HTLV-1-associated neurological disease. *Blood* 2008; 112:2411–20.
- Yashiki S, Fujiyoshi T, Arima N, et al. HLA-A*26, HLA-B*4002, HLA-B*4006, and HLA-B*4801 alleles predispose to adult T cell leukemia: the limited recognition of HTLV type 1 tax peptide anchor motifs and epitopes to generate anti-HTLV type 1 tax CD8(+) cytotoxic T lymphocytes. *AIDS Res Hum Retroviruses* 2001; 17:1047–61.
- Kozako T, Arima N, Toji S, et al. Reduced frequency, diversity, and function of human T cell leukemia virus type 1-specific CD8⁺ T cell in adult T cell leukemia patients. *J Immunol* 2006; 177:5718–26.
- Bunce M, O'Neill CM, Barnardo MC, et al. Phototyping: comprehensive DNA typing for HLA-A, B, C, DRB1, DRB3, DRB4, DRB5 &

- DQB1 by PCR with 144 primer mixes utilizing sequence-specific primers (PCR-SSP). *Tissue Antigens* **1995**; 46:355–67.
28. Betts MR, Brenchley JM, Price DA, et al. Sensitive and viable identification of antigen-specific CD8+ T cells by a flow cytometric assay for degranulation. *J Immunol Methods* **2003**; 281:65–78.
 29. Lee B, Tanaka Y, Tozawa H. Monoclonal antibody defining tax protein of human T-cell leukemia virus type-I. *Tohoku J Exp Med* **1989**; 157:1–11.
 30. Hanon E, Hall S, Taylor GP, et al. Abundant tax protein expression in CD4+ T cells infected with human T-cell lymphotropic virus type I (HTLV-I) is prevented by cytotoxic T lymphocytes. *Blood* **2000**; 95:1386–92.
 31. Kozako T, Yoshimitsu M, Fujiwara H, et al. PD-1/PD-L1 expression in human T-cell leukemia virus type 1 carriers and adult T-cell leukemia/lymphoma patients. *Leukemia* **2009**; 23: 375–82.
 32. Petrovas C, Price DA, Mattapallil J, et al. SIV-specific CD8+ T cells express high levels of PD1 and cytokines but have impaired proliferative capacity in acute and chronic SIVmac251 infection. *Blood* **2007**; 110:928–36.
 33. Kasagi S, Kawano S, Okazaki T, et al. Anti-programmed cell death 1 antibody reduces CD4+PD-1+ T cells and relieves the lupus-like nephritis of NZB/W F1 mice. *J Immunol* **2010**; 184:2337–47.
 34. Hokey DA, Johnson FB, Smith J, et al. Activation drives PD-1 expression during vaccine-specific proliferation and following lentiviral infection in macaques. *Eur J Immunol* **2008**; 38:1435–45.
 35. Petrovas C, Casazza JP, Brenchley JM, et al. PD-1 is a regulator of virus-specific CD8+ T cell survival in HIV infection. *J Exp Med* **2006**; 203:2281–92.
 36. Sieburg M, Tripp A, Ma JW, Feuer G. Human T-cell leukemia virus type 1 (HTLV-1) and HTLV-2 tax oncoproteins modulate cell cycle progression and apoptosis. *J Virol* **2004**; 78:10399–409.

Brief report

Kinetics and intracellular compartmentalization of HTLV-1 gene expression: nuclear retention of HBZ mRNAs

*Francesca Rende,^{1,2} *Ilaria Cavallari,¹ Alberto Corradin,³ Micol Silic-Benussi,¹ Frederic Toulza,⁴ Gianna M. Toffolo,³ Yuetsu Tanaka,⁵ Steven Jacobson,⁶ Graham P. Taylor,⁴ Donna M. D'Agostino,^{1,2} Charles R. M. Bangham,⁴ and Vincenzo Ciminale^{1,2}

¹Department of Oncology and Surgical Sciences, University of Padova, Padova, Italy; ²Istituto Oncologico Veneto-Istituto Di Ricovero e Cura a Carattere Scientifico, Padova, Italy; ³Department of Information Engineering, University of Padova, Padova, Italy; ⁴Department of Immunology, Imperial College, London, United Kingdom; ⁵Department of Immunology, Graduate School of Medicine, University of the Ryukyus, Okinawa, Japan; and ⁶Viral Immunology Section, Neuroimmunology Branch, National Institutes of Health, Bethesda, MD

Human T-cell leukemia virus type 1 (HTLV-1) codes for 9 alternatively spliced transcripts and 2 major regulatory proteins named Tax and Rex that function at the transcriptional and posttranscriptional levels, respectively. We investigated the temporal sequence of HTLV-1 gene expression in primary cells from infected patients using splice site-specific quantitative RT-PCR. The results in-

dicated a two-phase kinetics with the tax/rex mRNA preceding expression of other viral transcripts. Analysis of mRNA compartmentalization in cells transfected with HTLV-1 molecular clones demonstrated the strict Rex-dependency of the two-phase kinetics and revealed strong nuclear retention of HBZ mRNAs, supporting their function as noncoding transcripts. Mathematical modeling under-

scored the importance of a delay between the functions of Tax and Rex, which was supported by experimental evidence of the longer half-life of Rex. These data provide evidence for a temporal pattern of HTLV-1 expression and reveal major differences in the intracellular compartmentalization of HTLV-1 transcripts. (Blood. 2011;117(18):4855-4859)

Introduction

Human T-cell leukemia virus type 1 (HTLV-1) is the causative agent of adult T-cell leukemia-lymphoma (ATLL) and tropical spastic paraparesis/HTLV-1-associated myelopathy (TSP/HAM). HTLV-1 uses several strategies for controlling the expression of its genome, including the production of 9 alternatively spliced transcripts (Figure 1A).¹⁻⁶ Production of plus-strand transcripts is controlled by Tax at the level of transcription and by Rex at the level of nucleo-cytoplasmic export of unspliced and partially spliced mRNAs.^{7,8} Regulation of the minus-strand HBZ transcripts, which lack elements responsive to Rex, remains to be determined.

Current models suggest that plus-strand HTLV-1 mRNAs are expressed with a distinct timing during the course of the viral life cycle, with a switch from early (Rex-independent) to late (Rex-dependent) transcripts. Although early studies showed a qualitative switch among classes of HTLV-1 mRNAs (multiply spliced vs unspliced),⁹⁻¹² detection of this phenomenon with quantitative transcript-specific methods has proven difficult.¹³

To answer this question we used quantitative RT-PCR to quantify proviral expression during the spontaneous proviral reactivation observed in cells from infected patients. The results demonstrated a "two-phase" expression pattern. Using transfection of HTLV-1 molecular clones and subcellular RNA fractionation we

demonstrated the Rex-dependency of the two-phase kinetics and determined the compartmentalization of the individual mRNAs, showing that more than 90% of the HBZ mRNAs were retained in the nucleus. Mathematical modeling¹⁴ revealed the importance of a delay of Rex function compared with Tax, which was supported by experimental evidence of delayed accumulation and longer half-life of Rex.

Methods

Samples from HTLV-1-infected patients

Peripheral blood mononuclear cells (PBMCs) from ATLL and TSP/HAM patients were purified as in.¹⁵ Patients are described in supplemental Table 1 (available on the Blood Web site; see the Supplemental Materials link at the top of the online article). All samples were obtained from patients after informed consent in accordance with the Declaration of Helsinki, with approval from the Imperial College and King's College hospitals (London) Institutional Review Boards.

Plasmids, cells, and transfections

Plasmid pBS1-2-3 consists of the tax/rex cDNA (exons 1, 2, and 3 flanked by the 5' and 3' LTRs, from infectious molecular clone CS-HTLV-1¹⁶) inserted in pBluescript (Stratagene). Plasmid ACH-Rex knockout (KO) was

Submitted November 8, 2010; accepted February 27, 2011. Prepublished online as *Blood* First Edition paper, March 11, 2011; DOI 10.1182/blood-2010-11-316463.

*F.R. and I.C. contributed equally.

The online version of this article contains a data supplement.

The publication costs of this article were defrayed in part by page charge payment. Therefore, and solely to indicate this fact, this article is hereby marked "advertisement" in accordance with 18 USC section 1734.

© 2011 by The American Society of Hematology

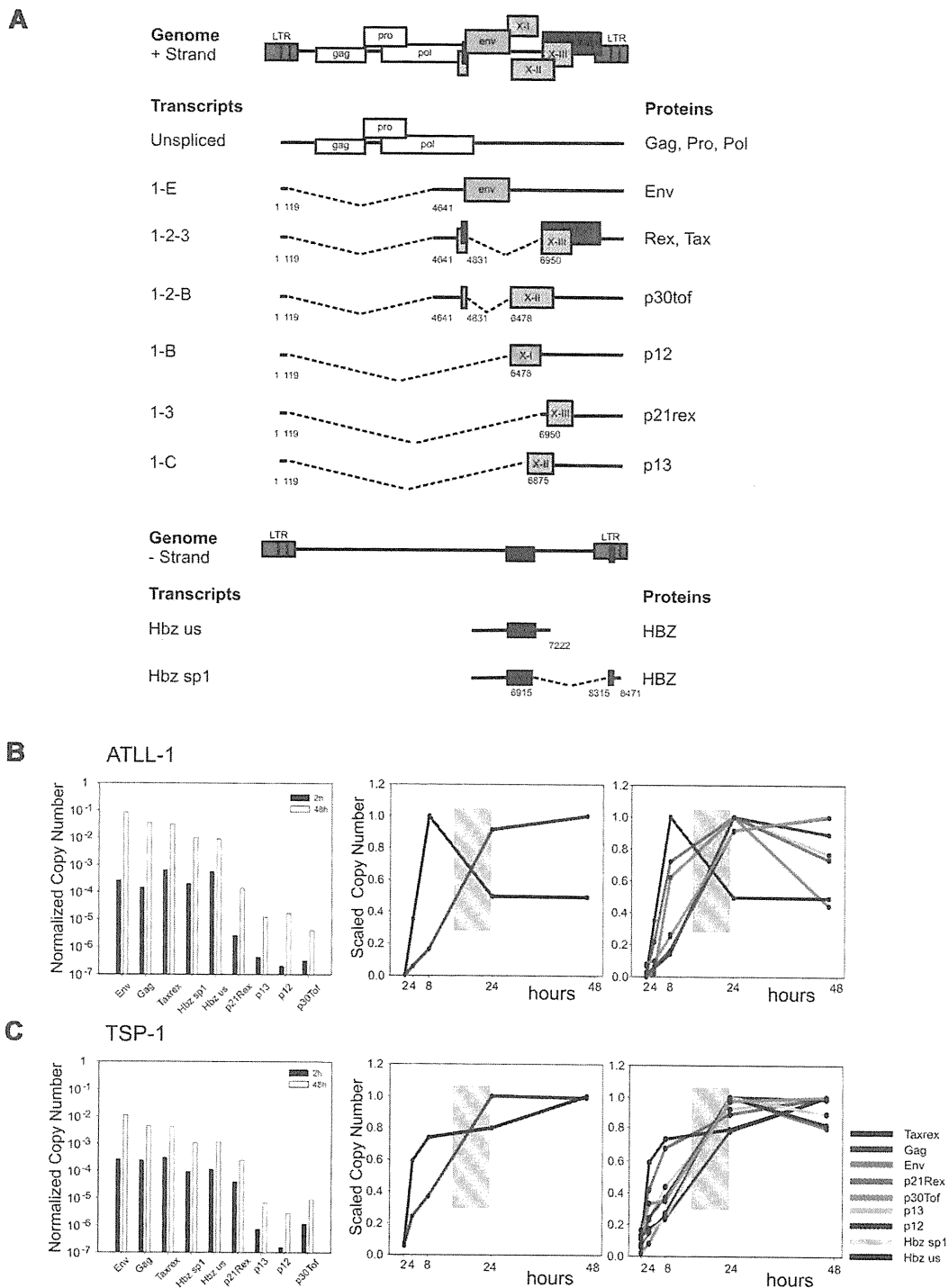


Figure 1. Temporal analysis of HTLV-1 expression in PBMCs from infected patients. (A) Structure and coding potential of plus- and minus-strand HTLV-1 mRNAs. (B-C) Bar graphs (left panels) show the Normalized Copy Numbers (NCN) of the indicated mRNAs after 2 hours (black bars) and 48 hours (white bars) of culture in vitro measured in representative ATLL and TSP/HAM patients; data on all patients studied are shown in supplemental Figure 1. NCN values were calculated by dividing the absolute copy number of each transcript by the absolute copy number of the 18S rRNA. Line graphs show the variation in the *tax/rex* and *gag* mRNAs (middle panels) and in all measured transcripts (right panels). Lines corresponding to *HBZ* mRNA are not shown for patient ATLL-1 because of insufficient material in the 8- and 24-hour time points. Scaled Copy Numbers (SCN) are plotted over a 48-hour time period (ie, at 2, 4, 8, 24, and 48 hours after depletion of CD8-positive cells and culture; cells were cultured in RPMI 1640 medium supplemented with 10% FCS, 2 mM glutamine, 100 IU/mL penicillin and 100 μ g/mL streptomycin). SCN values were calculated by dividing the NCN of each transcript at each time point by the maximum NCN value measured for that mRNA during the time course experiment. mRNAs are indicated by colors as shown in panel C right.

derived from the HTLV-1 molecular clone ACH¹⁷ by digestion with SphI followed by removal of 3' overhangs (including the Rex initiation codon) with T4 DNA polymerase and religation. Transfections were performed in the HeLa-derived cell line HLtat,¹⁸ chosen for its high transfection efficiency.

Quantitative RT-PCR

RNA of PBMCs from infected patients and transfected cells was extracted and viral transcripts were quantitated as detailed in supplemental Table 2.

Analysis of Tax and Rex expression

The time course of Tax and Rex expression was analyzed as described in Figure 2.

Results and discussion

Temporal analysis of HTLV-1 expression in PBMCs from infected patients

Although postulated based on the function of Tax and Rex,⁷ a temporal switch in HTLV-1 expression has not been demonstrated with quantitative transcript-specific methods. To investigate this possibility, we set up an *ex vivo* virus reactivation model based on the depletion of CD8⁺ T-cells from unstimulated PBMCs isolated from HTLV-1-infected patients, which reveals a sharp up-regulation of viral expression in the remaining PBMCs.¹⁵ Samples from 6 patients with TSP/HAM and 3 patients with ATLL were analyzed (supplemental Table 1). Splice-junction-specific Real-Time RT-PCR was used to measure the abundance (normalized copy number, NCN) and timing (scaled copy number, SCN) of expression of HTLV-1 transcripts (supplemental Table 2).

Figure 1 (B-C left) shows the NCN of the different mRNAs after 2 and 48 hours of culture *in vitro* (black bars and white bars, respectively) in representative cases of ATLL (patient ATLL-1) and TSP/HAM (patient TSP-1). Data on all patients studied are shown in supplemental Figure 1. Expression of all transcripts was substantially up-regulated on culture *in vitro*. The most abundant plus-strand transcripts were *tax/rax*, *gag* and *env*, followed by *p21rex*, *p30tof*, *p13* and *p12*; the minus-strand (HBZ) transcripts were readily detected.

Analysis of the timing of expression (SCN, Figure 1B-C middle) over a 48-hour time period showed that *tax/rax* was the earliest transcript followed by a rise in *gag* expression whose curve intersected that of *tax/rax* between 8 and 24 hours (indicated by a gray box in the figure), suggesting an “early-late” switch in HTLV-1 gene expression. Analysis of the SCN of all mRNAs (Figure 1B-C right) confirmed the “early-late” switch (gray box) and suggested a distinct temporal sequence of expression among the “late” mRNAs. The *p21Rex* mRNA was also detected as an early transcript in most samples, although its expression profile did not follow that of *tax/rax* in all the patients examined (see supplemental Figure 1).

Rex-dependence of the “two-phase” kinetics and nuclear retention of HBZ transcripts

The abundance and timing of expression of the HTLV-1 mRNAs were further investigated in cells transfected with the infectious HTLV-1 molecular clone ACH. This system permitted quantitation of transcripts in the cytoplasmic and nuclear fractions, which was not possible with patient samples because of limited amounts of material. Using a Rex knock-out derivative of ACH (ACH-Rex KO, Figure 2B right) we also tested the Rex-dependence of the two-phase expression kinetics.

Figure 2A (left) shows NCN in the cytoplasmic and nuclear fractions 24 hours after transfection of ACH. The most abundant plus-strand transcripts were *tax/rax* and *gag*, followed by *env* and *p21rex*; *p12*, *p13*, and *p30tof* were expressed at lower levels. The plus-strand transcripts showed similar partition in the nucleus and cytoplasm; in contrast the HBZ NCN was over 10-fold higher in the nucleus than in the cytoplasm.

The timing of expression was investigated by calculating “Export Ratios” over 48 hours (Figure 2B left). Consistent with results obtained from patient PBMCs (see preceding paragraph), ACH showed a two-phase expression kinetics with “early” *tax/rax* expression (measured as a sharp increase in export ratio) followed by a rise in the export ratios of the *gag* and *env* mRNAs. Importantly, the two-phase kinetics was abolished in cells expressing ACH-Rex KO (Figure 2B middle), demonstrating the critical role of Rex in regulating these kinetics. The export ratios of HBZ transcripts remained remarkably low throughout the time course and were not affected by Rex (Figure 2B left and middle). The nuclear retention of HBZ transcripts was also confirmed in the infected cell line C91PL¹⁹ (Figure 2A right). Although the significance of the nuclear retention of HBZ mRNAs remains to be understood, we propose that it might favor viral persistence by reducing HBZ translation thereby reducing exposure of the infected cell to the HBZ-specific host CD8⁺ T-cell response^{20,21} while allowing its function as a noncoding transcript driving T-cell proliferation.²²

Kinetics of Tax and Rex protein turnover

Mathematical modeling (supplemental Figure 2) underscored the importance of a delay in Rex function compared with Tax in the observed expression kinetics. These considerations led us to investigate the time course of Tax and Rex expression from plasmid pBS1–2-3, which expresses the full-length mature *tax/rax* mRNA (Figure 2C), and from the ACH molecular clone (Figure 2D). Flow cytometry analyses showed a relative accumulation of Rex at later time points (32, 48 hours) resulting in a progressive rise in the Rex/Tax ratio (right panels).

Consistent with these observations, a comparison of the half-lives of Tax and Rex expressed from pBS1–2-3 after treatment with cycloheximide revealed a slower rate of degradation of Rex compared with Tax (Figure 2E), with half-lives of 19.6 hours and 6.6 hours, respectively; similar half-lives were measured in ACH-transfected cells (data not shown). These findings provide experimental grounds for the delay in Rex function postulated in the mathematical model and suggest a posttranslational control of Tax and Rex activity.

Acknowledgments

We thank Luigi Chieco-Bianchi for discussions.

This work was supported by grants from the European Union (“The role of chronic infections in the development of cancer,” contract no. 2005-018704), the Associazione Italiana per la Ricerca sul Cancro (AIRC), the Fondazione Cariverona, the Ministero per l’Università e la Ricerca Scientifica, e Tecnologica Progetti di Ricerca di Interesse Nazionale (PRIN), the Ministero della Salute (project RFPS-2006-2-342-010), and the University of Padova.

Authorship

Contribution: F.R. and I.C. carried out transfections, immunoblotting and real-time RT-PCR assays; M.S.B. carried out flow cytometry analyses; G.P.T. provided patient samples and was responsible for all aspects of diagnosis and clinical management of the patients; C.R.M.B., F.T., and S.J. helped design and set up the assays to measure HTLV-1 mRNAs in cells from infected

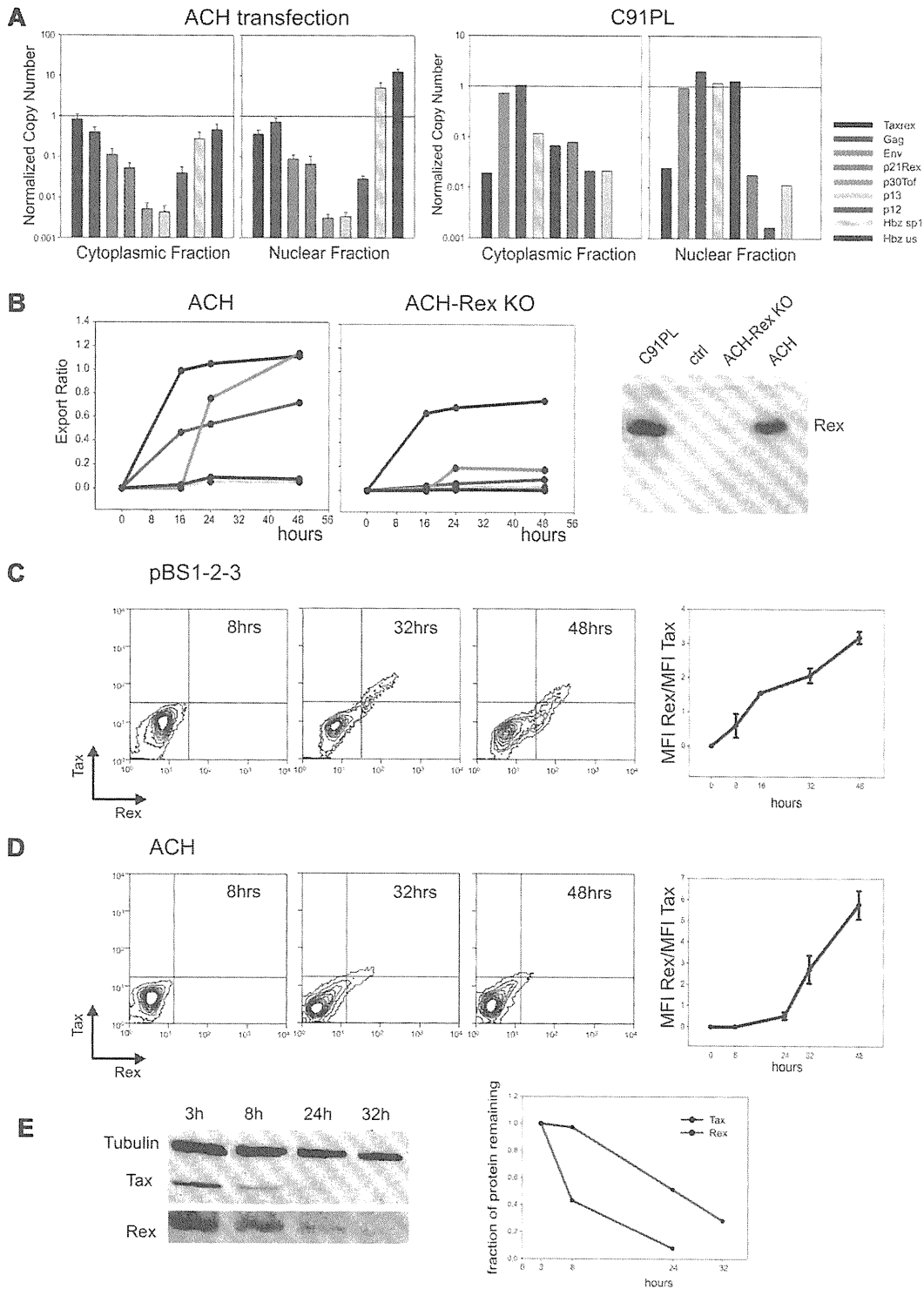


Figure 2. Kinetics and intracellular compartmentalization of HTLV-1 mRNAs; temporal analysis of Tax and Rex protein turnover. (A left) NCN of all HTLV-1 mRNAs in the cytoplasmic and nuclear fractions 24 hours after transfection of HLTat cells with wild-type HTLV-1 molecular clone ACH using Fugene6 (Roche; mean of 3 experiments, standard error bars). NCN values were determined by dividing the absolute copy number of each transcript by the absolute copy number of the *GAPDH* mRNA. (Right) NCN of all HTLV-1 mRNAs in the cytoplasmic and nuclear fractions of the chronically infected cell line C91PL.¹⁹ (B) Kinetic analysis of the nucleo-cytoplasmic export of the *tax/rax*, *gag*, *env* and *HBZ* mRNAs expressed from ACH (left) and ACH-Rex-KO (middle) in transfected HLTat cells. RNA was extracted from nuclear and cytoplasmic fractions using the Paris Kit (Ambion). "Export Ratios" were calculated as the ratio between cytoplasmic and total NCN over a time course of 48 hours (harvesting at 0, 16, 24, and 48 hours). The right panel shows Western blot analysis to detect Rex protein (see description in panel E); results verified that the ACH-Rex-KO does not express Rex. (C) Kinetics of Tax and Rex protein expression in HLTat cells from plasmid pBS1-2-3, which contains the viral 5' and 3' LTRs and expresses the full-length *tax/rax* mRNA (including all coding and noncoding regions). Cultures were harvested at 8, 16, 32, and 48 hours after transfection. Cells were fixed in 3.7% formaldehyde-PBS, permeabilized in 0.2% Triton-PBS, blocked with 3% BSA (bovine serum albumin)-PBS and then incubated for 1 hour with mouse anti-Tax monoclonal antibody²³ (1:100, in PBS-1.5% BSA) and rabbit anti-Rex polyclonal antibody²⁴ (1:500, in PBS-1.5% BSA). Cells were next incubated for 1 hour with Alexa 633-conjugated goat anti-mouse and Alexa 488-conjugated chicken anti-rabbit antibodies (Molecular Probes) diluted 1:1000 in PBS-1.5% BSA. Tax and Rex protein expression was analyzed by flow cytometry using a FACSCalibur (Becton Dickinson) equipped with 633-nm Helium-Neon and 488-nm Argon lasers. Alexa 633 and Alexa 488 fluorescent signals were analyzed using the FL4 (661 ± 16 nm) and the FL1 (530 ± 30 nm) detection lines, respectively. Data are represented as equal probability plots. The line graph (right) shows mean and standard error values of Rex/Tax

Figure 2. (continued) fluorescence intensity (mean fluorescence value X number of positive events) ratios measured in 3 independent experiments. (D) Kinetics of Tax and Rex protein expression in HLt cells from the infectious HTLV-1 molecular clone ACH. Cultures were harvested at 8, 24, 32, and 48 hours after transfection. Cells were processed and analyzed as described for panel C. Data are represented as equal probability plots. The line graph (right) shows mean and standard error values of Rex/Tax fluorescence intensity (mean fluorescence value X number of positive events) ratios measured in 3 independent experiments. (E) Degradation rates of the Tax and Rex protein expressed from pBS1–2-3 after blocking protein synthesis. HLt cells transfected with pBS1–2-3 were treated with 10 μ M cycloheximide 24 hours after transfection and harvested in “disruption buffer” (Paris kit; Ambion) at 3, 8, 24, and 32 hours after cycloheximide treatment. Lysates were subjected to SDS-PAGE and electrotransferred to Hybond-C Extra (GE Healthcare). Blots were incubated with mouse anti-Tax monoclonal antibody (1:500), rabbit anti-Rex polyclonal antibody (1:5000) and mouse anti-tubulin monoclonal antibody (1:2000) in PBS-3% BSA-0.05% Tween followed by a horseradish peroxidase-conjugated anti-mouse or anti-rabbit antibody (Pierce) diluted 1:5000 in 2% milk (Roche)–PBS-0.05% Tween. Blots were developed using chemiluminescence reagents (Supersignal, Pierce) and immunoreactive bands were visualized and quantified using a BioRad ChemiDoc XRS imager. The left panel shows a composite of this Western blot analysis to detect the Tax, Rex and Tubulin signals. Data were normalized by dividing Tax and Rex signals by the tubulin signal and scaled against the value at 3 hours; resulting numbers, which represented the fraction of protein remaining, were plotted in the graph on the right. Protein half-life was estimated by fitting a linear decay model to the data, assuming a constant degradation rate.

patients; D.M.D. and V.C. designed the experiments and prepared the manuscript; G.M.T. and A.C. developed the mathematical models of HTLV-1 expression; Y.T. provided Tax-specific antibodies; and all authors contributed to the analysis and interpretation of the data.

Conflict-of-interest disclosure: The authors declare no competing financial interests.

Correspondence: Vincenzo Ciminale, Dipartimento di Scienze Oncologiche e Chirurgiche, Università di Padova, Via Gattamelata 64, I-35128 Padova, Italy; e-mail: v.ciminale@unipd.it.

References

- Ciminale V, Pavlakis GN, Derse D, Cunningham CP, Felber BK. Complex splicing in the human T-cell leukemia virus (HTLV) family of retroviruses: novel mRNAs and proteins produced by HTLV type I. *J Virol*. 1992;66(3):1737-1745.
- Berneman ZN, Gartenhaus RB, Reitz MS Jr, et al. Expression of alternatively spliced human T-lymphotropic virus type I pX mRNA in infected cell lines and in primary uncultured cells from patients with adult T-cell leukemia/lymphoma and healthy carriers. *Proc Natl Acad Sci U S A*. 1992; 89(7):3005-3009.
- Koralnik IJ, Gessain A, Klotman ME, Lo Monaco A, Berneman ZN, Franchini G. Protein isoforms encoded by the pX region of human T-cell leukemia/lymphotropic virus type I. *Proc Natl Acad Sci U S A*. 1992;89(18):8813-8817.
- Cereseto A, Berneman Z, Koralnik I, Vaughn J, Franchini G, Klotman ME. Differential expression of alternatively spliced pX mRNAs in HTLV-I-infected cell lines. *Leukemia*. 1997;11(6):866-870.
- Princler GL, Julias JG, Hughes SH, Derse D. Roles of viral and cellular proteins in the expression of alternatively spliced HTLV-1 pX mRNAs. *Virology*. 2003;317(1):136-145.
- Matsuoka M. HTLV-1 bZIP factor gene: its roles in HTLV-1 pathogenesis. *Mol Aspects Med*. 2010; 31(5):359-66.
- Lairmore M, Franchini G. Human T-cell leukemia virus types 1 and 2. In: Knipe DM, Howley PM, et al, eds. *Fields Virology, Fifth Edition*. Vol 2. Philadelphia, PA: Lippincott Williams and Wilkins; 2007:2071-2106.
- Younis I, Green PL. The human T-cell leukemia virus Rex protein. *Front Biosci*. 2005;10:431-445.
- Hidaka M, Inoue J, Yoshida M, Seiki M. Post-transcriptional regulator (rex) of HTLV-1 initiates expression of viral structural proteins but suppresses expression of regulatory proteins. *EMBO J*. 1988;7(2):519-523.
- Grone M, Koch C, Grassmann R. The HTLV-1 Rex protein induces nuclear accumulation of unspliced viral RNA by avoiding intron excision and degradation. *Virology*. 1996;218(2):316-325.
- Inoue J, Itoh M, Akizawa T, Toyoshima H, Yoshida M. HTLV-1 Rex protein accumulates unspliced RNA in the nucleus as well as in cytoplasm. *Oncogene*. 1991;6(10):1753-1757.
- Dokhelar MC, Pickford H, Sodroski J, Haseltine WA. HTLV-1 p27^{rex} regulates gag and env protein expression. *J Acquir Immune Defic Syndr*. 1989; 2(5):431-440.
- Li M, Kesic M, Yin H, Yu L, Green PL. Kinetic analysis of human T-cell leukemia virus type 1 gene expression in cell culture and infected animals. *J Virol*. 2009;83(8):3788-3797.
- Corradin A, DIC B, Rende F, Ciminale V, Toffolo GM, Cobelli C. Retrovirus HTLV-1 gene circuit: a potential oscillator for eukaryotes. *Pac Symp Biocomput*. 2010:421-432.
- Hanon E, Hall S, Taylor GP, et al. Abundant tax protein expression in CD4+ T cells infected with human T-cell lymphotropic virus type I (HTLV-I) is prevented by cytotoxic T lymphocytes. *Blood*. 2000;95(4):1386-1392.
- Derse D, Mikovits J, Polianova M, Felber BK, Ruscetti F. Virions released from cells transfected with a molecular clone of human T-cell leukemia virus type I give rise to primary and secondary infections of T cells. *J Virol*. 1995;69(3):1907-1912.
- Kimata JT, Wong FH, Wang JJ, Ratner L. Construction and characterization of infectious human T-cell leukemia virus type 1 molecular clones. *Virology*. 1994;204(2):656-664.
- Schwartz S, Felber BK, Benko DM, Fenyo EM, Pavlakis GN. Cloning and functional analysis of multiply spliced mRNA species of human immunodeficiency virus type 1. *J Virol*. Jun. 1990; 64(6):2519-2529.
- MacNamara A, Rowan A, Hilburn S, et al. HLA class I binding of HBZ determines outcome in HTLV-1 infection. *PLoS Pathog*. 2010;6(9): pii: e1001117.
- Hilburn S, Rowan A, Demontis MA, et al. In vivo expression of human T-lymphotropic virus type 1 basic leucine-zipper protein generates specific CD8+ and CD4+ T-lymphocyte responses that correlate with clinical outcome. *J Infect Dis*. 2011; 203(4):529-536.
- Satou Y, Yasunaga J, Yoshida M, Matsuoka M. HTLV-I basic leucine zipper factor gene mRNA supports proliferation of adult T cell leukemia cells. *Proc Natl Acad Sci U S A*. 2006;103(3): 720-725.
- Popovic M, Lange-Wantzin G, Sarin PS, Mann D, Gallo RC. Transformation of human umbilical cord blood T cells by human T-cell leukemia/lymphoma virus. *Proc Natl Acad Sci U S A*. 1983; 80(17):5402-5406.
- Lee B, Tanaka Y, Tozawa H. Monoclonal antibody defining tax protein of human T-cell leukemia virus type-I. *Tohoku J Exp Med*. 1989;157(1):1-11.
- Bhat NK, Adachi Y, Samuel KP, Derse D. HTLV-1 gene expression by defective proviruses in an infected T-cell line. *Virology*. 1993;196(1):15-24.

Review Article

Immunopathogenesis of Human T-Cell Leukemia Virus Type-1-Associated Myelopathy/Tropical Spastic Paraparesis: Recent Perspectives

Mineki Saito¹ and Charles R. M. Bangham²

¹Department of Immunology, Graduate School of Medicine, University of the Ryukyus, 207 Uehara, Okinawa 903-0215, Japan

²Department of Immunology, Wright-Fleming Institute, Imperial College London, Norfolk Place, London W2 1PG, UK

Correspondence should be addressed to Mineki Saito, mineki@med.u-ryukyu.ac.jp

Received 1 August 2011; Revised 30 September 2011; Accepted 9 October 2011

Academic Editor: Pooja Jain

Copyright © 2012 M. Saito and C. R. M. Bangham. This is an open access article distributed under the Creative Commons Attribution License, which permits unrestricted use, distribution, and reproduction in any medium, provided the original work is properly cited.

Human T-cell leukemia virus type-1 (HTLV-1) is a replication-competent human retrovirus associated with two distinct types of disease only in a minority of infected individuals: the malignancy known as adult T-cell leukemia (ATL) and a chronic inflammatory central nervous system disease HTLV-1-associated myelopathy/tropical spastic paraparesis (HAM/TSP). HAM/TSP is a chronic progressive myelopathy characterized by spastic paraparesis, sphincter dysfunction, and mild sensory disturbance in the lower extremities. Although the factors that cause these different manifestations of HTLV-1 infection are not fully understood, accumulating evidence from host population genetics, viral genetics, DNA expression microarrays, and assays of lymphocyte function suggests that complex virus-host interactions and the host immune response play an important role in the pathogenesis of HAM/TSP. Especially, the efficiency of an individual's cytotoxic T-cell (CTL) response to HTLV-1 limits the HTLV-1 proviral load and the risk of HAM/TSP. This paper focuses on the recent advances in HAM/TSP research with the aim to identify the precise mechanisms of disease, in order to develop effective treatment and prevention.

1. Introduction

Human T-cell leukemia virus type-1 (HTLV-1) is a human retrovirus etiologically associated with adult T-cell leukemia (ATL) [1–3] and HTLV-1-associated myelopathy/tropical spastic paraparesis (HAM/TSP) [4, 5]. HAM/TSP is a chronic progressive myelopathy characterized by spastic paraparesis, sphincter dysfunction, and mild sensory disturbance in the lower extremities [6]. Cases of HAM/TSP have been reported throughout the HTLV-1 endemic areas such as Southern Japan, the Caribbean, Central and South America, the Middle East, Melanesia, and equatorial regions of Africa [7]. Sporadic cases have also been described in nonendemic areas such as the United States and Europe, mainly in immigrants from an HTLV-1 endemic area. In contrast to HIV-1 infection, few with HTLV-1 develop disease: approximately 2%–3% of infected persons develop ATL [8] and other 0.25%–3.8% develop HAM/TSP [9–12], while

the majority of infected individuals remain lifelong asymptomatic carriers (ACs). However, the ability to evaluate the individual risk of HTLV-1-associated diseases in each AC would make a significant clinical impact, especially in HTLV-1 endemic areas. During the last three decades since the discovery of HTLV-1 as the first pathogenic human retrovirus, advances in HTLV-1 research have helped us to understand the clinical features of HTLV-1 associated diseases, the virological properties of HTLV-1, and the importance of the viral, host, and environmental risk factors as well as the host immune response against HTLV-1 infection. However, the precise mechanism of disease pathophysiology is still incompletely understood, and the treatment is still unsatisfactory, because good small-animal models for studying HTLV-1 infection and its associated diseases were unavailable until recently. In this paper, we summarize the recent developments of HTLV-1 research to try to identify more precisely the pathogenetic mechanisms

of the disease in order to develop effective treatment and prevention.

2. HTLV-1 Infection and Clinical Features of HAM/TSP

2.1. Virological Aspects of HTLV-1. HTLV-1 is classified as a complex retrovirus in the genus *Deltaretrovirus* of the subfamily *Orthoretrovirinae* and infects 10–20 million people worldwide [13–15]. HTLV-1 can be transmitted through sexual contact [16], injection drug use [15], and breastfeeding from mother to child [17, 18]. For over two decades, the investigation of HTLV-1-mediated pathogenesis has been focused on Tax, an HTLV-1 encoded viral oncoprotein, since Tax has been viewed as critical for leukemogenesis because of its pleiotropic effects on both viral and many cellular genes responsible for cell proliferation, genetic instability, dysregulation of the cell cycle, and apoptosis [19]. However, Tax expression is not detected in about 60% of freshly isolated samples from ATL cases [20]. In 2002, another regulatory protein encoded in the minus or antisense strand of the virus genome, named HTLV-1 basic leucine zipper factor (HBZ), was identified [21]. The spliced form of HBZ is expressed in all ATL [22] and HAM/TSP [23] cases, and its expression is strongly correlated with the HTLV-1 proviral load (PVL) in HTLV-1-infected individuals and with disease severity in HAM/TSP patients [23]. Also, HBZ protein promotes proliferation of ATL cells and induces T-cell lymphomas in CD4⁺ T cells by transgenic expression, indicating the possible involvement of HBZ expression in the development of ATL [22, 24]. Moreover, among the HTLV-1 encoded viral genes, only the HBZ gene sequence remains intact, unaffected by nonsense mutations and deletion [25]. These findings indicate that HBZ expression is indispensable for proliferation and survival of ATL cells and HTLV-1 infected cells, and that Tax expression is not always necessary for the maintenance of ATL [26].

2.2. Clinical and Pathological Features of HAM/TSP. HAM/TSP is a chronic progressive myelopathy characterized by spastic paraparesis, sphincter dysfunction, and mild sensory disturbance in the lower extremities [6]. In addition to neurological symptoms, some HAM/TSP cases also exhibit autoimmune-like disorders, such as uveitis, arthritis, T-lymphocyte alveolitis, polymyositis, and Sjögren syndrome [14]. Among ACs, the lifetime risk of developing HAM/TSP, which is different among different ethnic groups, ranges between 0.25% and 4%. It has been reported that the annual incidence of HAM/TSP is higher among Jamaican subjects than among Japanese subjects (20 versus 3 cases/100,000 population), with a two to three times higher risk for women in both populations [9–12]. The period from initial HTLV-1 infection to the onset of HAM/TSP is assumed to range from months to decades, a shorter time than for ATL onset [11, 31]. HAM/TSP occurs both in vertically infected individuals and in those who become infected later in life (i.e., through sexual contact [almost exclusively from male to female], intravenous drug use, contaminated blood transfusions, etc.). The mean age at onset is 43.8 years, and

the frequency of HAM/TSP is higher in women than in men (the male to female ratio of occurrence is 1 : 2.3) [11].

Pathological analysis of HAM/TSP autopsy materials indicates that the disease affects the spinal cord, predominantly at the thoracic level [27, 32, 33]. Loss of myelin and axons in the lateral, anterior, and posterior columns is associated with perivascular and parenchymal lymphocytic infiltration with the presence of foamy macrophages, proliferation of astrocytes, and fibrillary gliosis. In the cases with active-chronic lesions in the spinal cord, perivascular inflammatory infiltration with similar composition of cell subsets was also seen in the brain [28]. The peripheral nerve pathology of HAM/TSP patients with sensory disturbance showed varying degrees of demyelination, remyelination, axonal degeneration, regeneration, and perineurial fibrosis [29, 30]. The presence of atypical lymphocytes (so-called “flower cells”) in peripheral blood and cerebrospinal fluid (CSF), a moderate pleocytosis, and raised protein content in CSF are typically found in HAM/TSP patients. Oligoclonal immunoglobulin bands in the CSF, raised concentrations of inflammatory markers such as neopterin, tumor necrosis factor (TNF)- α , interleukin (IL)-6 and interferon (IFN)- γ , and an increased intrathecal antibody (Ab) synthesis specific for HTLV-1 antigens have also been described [34]. Clinical progression of HAM/TSP is associated with an increase in the proviral load in individual patients, and a high ratio of proviral loads in CSF cells/peripheral blood mononuclear cells (PBMCs) is also significantly associated with clinically progressive disease [35]. The clinical and pathological characteristics of HAM/TSP described above are shown in Table 1.

3. Risk Factors for HAM/TSP

3.1. Host Genetic. A previous population association study of 202 cases of HAM/TSP and 243 ACs in Kagoshima prefecture, HTLV-1 endemic Southern Japan, revealed that one of the major risk factors is the HTLV-1 PVL. The median PVL was more than ten times higher in HAM/TSP patients than in ACs, and a high PVL was also associated with an increased risk of progression to disease [36, 37]. A higher PVL in HAM/TSP patients than in ACs was observed in other endemic areas such as the Caribbean [38], South America [39], and the Middle East [40]. It was suggested that genetic factors such as the human leukocyte antigen (HLA) genotype are related to the high PVL in HAM/TSP patients and genetic relatives. In Southern Japan, possession of the HLA-class I genes HLA-A*02 and Cw*08 was associated with a statistically significant reduction in both HTLV-1 PVL and the risk of HAM/TSP, whereas possession of HLA-class I HLA-B*5401 and class II HLA-DRB1*0101 predisposes to HAM/TSP in the same population (Table 2) [37, 41]. Since the function of class I HLA proteins is to present antigenic peptides to CTL, these results imply that individuals with HLA-A*02 or HLA-Cw*08 mount a particularly efficient CTL response against HTLV-1, which may therefore be an important determinant of HTLV-1 PVL and the risk of HAM/TSP. In fact, it has been reported that CTL spontaneously kills autologous HTLV-1-infected